THE CRYSTAL AND MOLECULAR STRUCTURES OF $(C_5H_5)_2Cr_2(NO)_3(NH_2)$, $KIO_3.HIO_3$, α-$(CH_3)_2TeI_2$ and $(CH_3)_2AsC{=}CAs(CH_3)_2CF_2CF_2Mn_2(CO)_8$

by

LILIAN YAN YAN CHAN

B.Sc. University of Hong Kong , 1967

A DISSERTATION SUBMITTED IN PARTIAL FULFILLMENT

OF THE REQUIREMENTS FOR THE DEGREE OF

DOCTOR OF PHILOSOPHY

in the Department

of

Chemistry

SIMON FRASER UNIVERSITY

September, 1971

APPROVAL

Name: Lilian Yan Yan Chan

Degree: Doctor of Philosophy

Title of Thesis: The Crystal and Molecular Structures of

$(C_5H_5)_2Cr_2(NO)_3(NH_2)$, $KIO_3.HIO_3$, α-$(CH_3)_2TeI_2$

and $(As(CH_3)_2)_2\overline{C=CCF_2CF_2}Mn_2(CO)_8$

Examining Committee:

F.W.B.Einstein
Senior Supervisor

A.C.Oehlschlager
Examining Committee

D.Sutton
Examining Committee

D.G.Tuck
Examining Committee

J.Trotter
External Examiner
Department of Chemistry
University of British Columbia

Date Approved: October 20, 1971.

Abstract

The crystal structures of four inorganic compounds: $(C_5H_5)_2Cr_2(NO)_3(NH_2)$ (I), $KIO_3.HIO_3$ (II), α-$(CH_3)_2TeI_2$ (III), and $(CH_3)_2AsC{=}CAs(CH_3)_2CF_2CF_2Mn_2(CO)_8$ (abbrev. as $f_4farsMn_2(CO)_8$) (IV), were determined by x-ray diffraction techniques. Intensity data collection was carried out on a Picker four-circle diffractometer, manually operated for (I) and (II), and computer controlled for (III) and (IV). While the Phase Problem in (II) and (IV) was solved by Patterson synthesis, that in (III) was solved by Direct Methods (Tangent Refinement Program). The structure solution of (I) was complicated by the existence of pseudo-symmetry and was solved by using Direct Methods (Symbolic Addition Procedure). Refinement of the atomic and thermal parameters in all cases was by full-matrix least-squares techniques. Results are shown in the following table:

compounds	I	II	III	IV
number of reflexions measured	903	1644	3157	1580
number of reflexions regarded as significantly above background (N)	511	1392	2197	1439
no. of variables (V)	77	94	107	208
N/V	6.6	14.8	20.5	6.9
final R-value (%)	6.9	5.0	5.4	3.5

The thesis also gives a discussion of the significance of the results and a detailed description of the experimental and computing methods used in the structure determination of these compounds. The following briefly describes the major features in each structure.

In (I), the two chromium atoms are linked together by a chromium-chromium bond (2.650(4)Å) and by bridging nitrosyl and amido groups, each chromium atom is also bonded to a terminal nitrosyl group and a π-cyclopentadiene ring. In this model of the structure, a crystallographic mirror plane passes through the Cr-Cr bond and the terminal nitrosyl groups with the two bridging groups being disordered. Each cyclopentadiene ring is described by two equal occupancy disordered orientations.

In (II), the iodate groups are primarily trigonal pyramidal. Weak interionic (I...O) and hydrogen (OH...O) bonds result in a three-dimensional network with a corresponding increase in the coordination numbers (six and seven) about the iodine atoms. Significant differences are found between the I-O and I-OH bonds.

In (III), each tellurium atom in the molecule has a distorted octahedral environment formed by two trans- Te-I, two cis- Te-C covalent bonds and two short intermolecular Te...I contacts from iodine atoms attached to neighbouring $(CH_3)_2TeI_2$ molecules. As a result, the

molecules are linked together in corrugated sheets. Since there are three crystallographically distinct $(CH_3)_2TeI_2$ molecules in the asymmetric unit, variations in the Te-I bonds can be correlated with the regularity of the octahedral environment about the tellurium atoms.

In (IV), the molecule is binuclear ; each manganese atom is bonded to an arsenic atom and four carbonyl groups. The two $Mn(CO_4)$ units are joined together by a long Mn-Mn bond (2.971(3) Å) and the bridging $f_4$fars ligand. The molecule is twisted about the Mn-Mn bond so that the ligands of the two manganese atoms are almost perfectly staggered, as in the parent compound $Mn_2(CO)_{10}$.

To Tin and my parents

TABLE OF CONTENTS

LIST OF TABLES

LIST OF FIGURES

ACKNOWLEDGMENT

I would like to express my gratitude to my Research Director Dr.F.W.B.Einstein for his most helpful advice and guidance throughout this work.

My sincere thanks are also extended to:

Dr. N.Flitcroft for a sample of $(C_5H_5)_2Cr_2(NO)_3(NH_2)$;

Dr. W.R.Cullen for a sample of $f_4farsMn_2(CO)_8$;

Drs F.R.Ahmed and B.R.Penfold for computer programs;

Mrs. Misa Gratton for computing assistance;

The faculty, staff and students of the Chemistry Department at S.F.U. for helpful discussions and suggestions;

My girl friends for helping to type the manuscript of this dissertation;

My husband Tin and Dr.F.W.B.Einstein for helping to proof-read the manuscript of this dissertation;

And the National Research Council of Canada for financial support and the award of a Post-Graduate Scholarship.

CHAPTER 1

INTRODUCTION

X-ray diffraction techniques have been most valuable in providing quantitative data from structural studies in the solid state. Moreover the development of computers in recent years has had great impact on the technical aspect of structure determinations. This thesis describes the x-ray crystal structure analysis of four inorganic compounds: dicyclopentadienyldinitrosyl-μ-nitrosyl-μ-amidodichromium(I), $(C_5H_5)_2Cr_2(NO)_3(NH_2)$ (I); potassium hydrogen di-iodate, $KIO_3.HIO_3$ (II); α-dimethyltellurium di-iodide, α-$(CH_3)_2TeI_2$ (III); and tetrafluorocyclobutenebis(dimethylarsine)-octacarbonyldimanganese(0), $(CH_3)_2AsC{=}CAs(CH_3)_2CF_2CF_2Mn_2(CO)_8$ (abbreviated as $f_4farsMn_2(CO)_8$) (IV).

Displacement of chloride from cyclopentadienyl-dinitrosyl-chloro-chromium, $(C_5H_5)Cr(NO)_2Cl$, can lead to mononuclear or binuclear products. The binuclear products containing bridging groups attracted attention as several geometrical isomers were possible[1]. The structures of $[C_5H_5Cr(NO)_2]_2$ [2] both in solid and liquid states would be interesting as they can be compared with the analogous complexes, e.g. $[C_5H_5Fe(NO)_2]_2$[3], which exhibit geometric isomerism.[3,4] It had been reported that during the preparation

of $[C_5H_5Cr(NO)_2]_2$, a by-product, compound (I), was obtained[5], presumably formed by the reduction of Cr-NO to $Cr-NH_2$ by $NaBH_4$. From spectroscopic evidence it was expected to have unusual mixed amido and nitrosyl bridges as well as a possible metal-metal bond. Until 1969 there was no report on crystal structures of compounds with bridging nitrosyl groups. The chemical interest coupled with its stability in air and under x-rays made (I) an attractive subject for a crystal structure study.

During the infra-red studies of some iodate compounds it was found[6] that the spectrum for $KIO_3.HIO_3$ (II) was complex and the bands could not be assigned satisfactorily from a simple structural model. It was concluded that perhaps two kinds of iodate groups were present. It is interesting to note that various iodate compounds[7] possess non-linear optical properties and they have various applications in the solid state. Most of them were found to have secondary intermolecular interactions besides the primary bonding arrangement of trigonal pyramidal IO_3^- groups. In particular, the crystal structure of α-iodic acid, α-HIO_3[8], showed additional hydrogen bonding to form infinite chains of the type ....HIO_3....HIO_3....HIO_3.... . The crystal structure of (II) was expected to reveal the different environments about the iodine atoms due to possible intermolecular I...O interactions as well as the nature of

the hydrogen OH...O bonding.

The study of dimethyltellurium di-iodide dates back to the 1920's when Vernon[9] suggested that it existed in α and β forms which he concluded to be cis- and trans- isomers of a square-planar structure. Subsequent investigation by Drew[10] suggested that they were actually covalent (α) and ionic (β) isomers. The ionic (β) form was confirmed by an x-ray structure determination to be $[Te(CH_3)_3^+]$ $[Te(CH_3)I_4^-]$[11]. Preliminary x-ray work on the α isomer[12] showed that there were twelve formula units per unit cell, and the simple molecular formula of $(CH_3)_2TeI_2$ was therefore questioned. A detailed structure analysis of the α isomer was thus carried out to study its exact nature and and to compare it with the β form.

The ligating properties of the 1,2-bis (dimethylarsine)-tetrafluorocyclobutene $(CH_3)_2AsC{=}CAs(CH_3)_2CF_2CF_2$ ($f_4$fars) have been well known[13]. It can act as a monodentate, bidentate, tridentate or bridging ligand. (IV) was prepared by Crow et al[14a] by reaction of $f_4$fars with dimanganese decacarbonyl. Spectroscopic evidence indicated a bridging $f_4$fars ligand and a Mn-Mn bond. Reaction of (IV) with iodine at room temperature resulted in rupture of the metal-metal bond to give $f_4$fars-$Mn_2I_2(CO)_8$. It had a $f_4$fars ligand bridge as the only linkage between the two $MnI(CO)_4$ moieties which were twisted about the Mn-As bonds to lie on either

side of the cyclobutene ring[14b]. It was considered interesting to find out the exact coordination about the manganese atoms in (IV) before the rupture of the Mn-Mn bond, and to compare it with the parent compound $Mn_2(CO)_{10}$[15] as well as other related $f_4$fars derivatives.

CHAPTER 2

EXPERIMENTAL

A general outline of the experimental method is presented in this section. A summary of the crystal data is included for comparison in Table (I).

Crystals of (I) and (IV) were supplied by Drs N.Flitcroft and W.R.Cullen respectively.(III) was available as a commercial product. (II) was prepared by mixing warm equimolar aqueous solutions of KIO_3 and HIO_3 and crystals of $KIO_3.HIO_3$ separated out on cooling.

2.1 Preliminary Examination and Photography

Samples of the crystals were examined with a hand-lens and under a polarizing microscope before mounting. Unlike the others which were stable in air, crystals of (III) were extremely volatile and toxic. They were therefore first examined inside a vial with the hand-lens and four suitable crystals were then individually sealed in capillaries. Since the single crystal fragment of (II) was a fragile, thin plate it was also sealed in a capillary. Suitable crystals of (I) and (IV) were mounted on thin glass fibres.

After a crystal was aligned on a two-circle Nonius Optical Goniostat, it was put on the Weissenberg and precession cameras to determine its quality, setting, cell dimensions

and possible space groups. The photographic information was specially helpful in (I) and (II)(as their intensity data were collected on a manually operated diffractometer)and served as input data to the program DSET2(written by E.L. Enwall) to calculate the angular settings for the unique set of reflexions.

The densities of the compounds were measured using a Berman density balance except in the case of (I) where a liquid of the same density was prepared and its density measured afterwards.

2.2 Diffractometry

In the cases of (I) (II) and (III), the single crystals for photography were also used for diffractometry. In the case of (IV), a crystal grinder was used to grind a crystal of cubic-size($\sim$ .5mm) very slowly to an approximate sphere of .17mm radius. To examine the quality and setting of this crystal before it was put on the diffractometer, a precession photograph was taken which was later identified to be the $\{hhl\}$ zone.

A manually operated Picker four-circle diffractometer was used for the data collection of (I) and (II) but it was fully-automated for (III) and (IV). The software was the Picker FACS I system for (III) and the Vanderbilt system (a modified version of FACS I by Dr. G. Lenhert, Vanderbilt University) for (IV). Differences in experimental procedures between (I) (II) and (III) (IV) thus mainly arose from the

manual and automatic operations of the diffractometer.

Two reflexions were carefully identified to determine the setting of a crystal. Both (I) and (II) had reciprocal axes at $\chi=90^{o}$ and $\chi=0^{o}$. (III) was mounted about the a (monoclinic) axis and both reflexions were aligned at $\chi=0^{o}$. The matrix for the general orientation of (IV) was calculated first from its photographically-determined cell dimensions and two carefully centred reflexions. Orientation matrices of (III) and (IV) were recalculated after accurate cell dimensions had been determined on the diffractometer. Since (III) and (IV) did not have reciprocal axes at $\chi=90^{o}$ the effects due to intrinsic multiple reflexion were minimized[6].

Accurate cell dimensions were determined from a least-squares fit to a number of reflexions whose 2θ values were accurately measured on the diffractometer. Unfiltered radiation and narrowed detector slit were used so that MoKα_1, α_2 and β positions could be distinctly resolved. MoKα_1 was used in (I),(III) and (IV) but all three radiations were used in (II) and a good consistency was found among the three results obtained. Measurements of both + and - 2θ were carried out in (I) and (II) and their average value was taken. In general the take-off angle was small to give a sharp-parallel incident beam in order to increase the accuracy of the measurement of the 2θ values.

Intensity data of the unique set of reflexions were

collected using the θ-2θ scan method. MoKα radiation ($\lambda = 0.7107\text{Å}$) was used with a niobium filter. The scan widths were determined by preliminary investigation of the mosaicity of the reflexions on the diffractometer prior to data collection. Scan widths were also corrected for dispersion effects in (III) and (IV). Since the diffraction spots as seen from the photographs of (I) and (II) were reasonably intense and sharp, a faster scan speed of 4°/min was used to accelerate manual data collection. A scan rate of 2°/min was used in (III) and (IV). Three standard reflexions were measured at least every four hours to check the consistency of the process and the fluctuations were ±1.5% (I), ±1.0%(II), ±2.5% (III) and ±2.3% (IV).

If absorption effects are not corrected, they can affect the accuracy of the results, particularly that of the thermal parameters. Since the linear absorption coefficients μ for (I) and (IV) were low giving only small variations of the transmission factors with θ and in their extreme values of μR (R=spherical radius of the crystal), no absorption corrections were applied. For (II) and (III) the values of μ were considerably higher. A semi-empirical method [17] of absorption correction

was used where the variation of intensity of a reflexion at $\chi=90^\circ$ was plotted against the azimuthal angle $\bar{\Phi}$. Relative transmission factors derived from the curve were applied to the intensity measured* according to the $\bar{\Phi}$ angles of the reflexions. The extreme variations of intensity due to absorption were about 3.0 in (II) and 2.0 in (III) and these reflexions involving extremely low transmission factors were few in number. This approximate absorption treatment was suitable for (II) as it was a thin plate and mounted in a direction parallel to the plate, but less ideal for (III) in terms of the crystal habit, where end effects could introduce errors and absorption correction might not be a function of $\bar{\Phi}$ alone. As the mounting of (III) gave no reflexion at $\chi=90^\circ$ during data collection, each arc on the goniometer head was moved by about 6° to give the reflexion 3 3 -1 at $\chi=90^\circ$.

* The reciprocals of the relative transmission factors are multiplied into the measured intensity

TABLE I. CRYSTAL DATA

		I	II	III	IV
formula		$(C_5H_5)_2Cr_2(NO)_3(NH_2)$	$KIO_3.HIO_3$	α-$Te(CH_3)_2I_2$	$f_4farsMn_2(CO)_8$
formula weight		340	390	411	448
colour		dark green	colourless	deep red	orange red
photography	Weissenberg	0kl-4kl(CrK_α)	h0l-h2l(CrK_α)	0kl-3kl(CrK_α)	0kl,1kl(CuK_α)
	Precession	hk0,h0l(MoK_α)	hk0,0kl and some general hkl(MoK_α)	h0l,0kl(MoK_α)	h0l,hk0(CuK_α) hhl
	systematic absences	0kl: k+l=2n+1 hk0: h=2n+1	h0l: l=2n+1 0k0: k=2n+1	same as (II)	0kl: k+l=2n+1 h0l: h=2n+1
space group		orthorhombic Pnma	monoclinic $P2_1/c$	same as (II)	orthorhombic $Pna2_1$
Dx-ray (gcm^{-3})		1.69	4.16	3.39	1.95
Dmeasured (gcm^{-3})		1.75	4.17	3.34 (reported [12])	1.97
Z		4	8	12	4
μMoK_α (cm^{-1})		17.6	108.7	113.9	23.8

(continued)

TABLE I. (CONTINUED)

Diffractometry

		I	II	III	IV
	crystal size and shape	.17x.36x.14 mm parallelpepid	.19x.54x.05 mm plate	.18x.33x.21 mm parallelpepid	.34mm diameter sphere
	mounting axis	a	b	a	general orientation
Accurate Determination of cell dimensions	no. of reflexions used	29	30	27	15
	temperature(°C)	21	22	21	23
	take-off angle(°)	1.3	1.2	1.2	0.7
	radiation used	$MoK\alpha_1$ (.70926Å)	$MoK\alpha_1$ (.70926Å), $K\alpha_2$ (.713543Å), $K\beta$ (.620990Å)	$MoK\alpha_1$	$MoK\alpha_1$
	cell dimensions a(Å)	7.948(4)	7.028(1)	9.439(1)	17.479(3)
	cell dimensions b(Å)	9.248(4)	8.203(1)	21.992(2)	12.713(3)
	cell dimensions c(Å)	17.489(6)	21.841(3)	12.217(1)	10.273(2)
	cell dimensions β(°)	90.0	98.03(1)	107.63(1)	90.0

(for $MoK\alpha_1$)

(continued)

TABLE I. (CONTINUED)

Diffractometry — Data Collection

	I	II	III	IV
scan width(°)	2.0	1.6	2.0(corrected for dispersion)	1.5(corrected for dispersion)
take-off angle(°)	1.3	1.2	1.2	4.3
rate of scan(°/min)	4.0	4.0	2.0	2.0
no. of independent reflexions measured	903	1644	3157	1580
operation	manual	manual	computer controlled FACS 1 system	computer controlled Vanderbilt system

CHAPTER 3

COMPUTATIONS

3.1 Data Reduction

3.1.1. The Structure Factor F

For a unit cell containing N atoms, the structure factor F is a function of the fractional coordinates (x_n, y_n, z_n), the scattering factor f_n and the temperature factor B_n of the nth atom as well as the Miller Indices h,k,l

$$F_{hkl} = \sum_{n=1}^{N} f_n e^{-B_n \sin^2\theta/\lambda^2} e^{[2\pi i(hx_n + ky_n + lz_n)]} \qquad (1)$$

where f_n in general can be written as the sum of the Rayleigh scattering (f_o), and the real ($\Delta f'$) and imaginary ($\Delta f''$) terms due to anomalous scattering:

$$f_n = f_o + \Delta f' + i\Delta f'' \qquad (2)$$

Although f_o is always the dominant factor, effects due to anomalous scattering should not be neglected. This point becomes particularly important when the structure is non-centrosymmetric, as illustrated in the structure determination of compound (IV) (section 3.6.4). The scattering factor curves used throughout this work, including anomalous scattering , were taken from the International Tables for x-ray crystallography[18] for the non-hydrogen atoms* and the paper by Stewart et al.[19] for the hydrogen atoms.

*SCF values for light atoms and TFD model values for atoms with atomic numbers larger than 23

3.1.2 The Intensity Equation

To find the atomic positions, one must be able to relate the structure factor F to the measured intensity I_{obs}. A single crystal of finite size will reflect over a certain angular range on either side of the Bragg angle θ given by:

$$\lambda = 2 d \sin\theta \qquad (3)$$

where λ is the wavelength and d is the interplanar spacing. If the crystal is turned through the reflecting position with angular velocity ω to give a total measured reflected energy E, the following equation[20] holds for a small crystal of ideal mosaicity:

$$\frac{E\omega}{I_o} = \left\{\frac{N' e^2}{m c^2}\right\}^2 (F F^*) \lambda^3 L p V A^{-1} \qquad (4)$$

where I_o = incident beam intensity (in energy/cm^2/sec)

N' = number of unit cells per unit volume of the crystal

m = mass of an electron

e = charge of an electron

c = velocity of light

L = Lorentz correction term

p = polarization correction term

V = volume of the crystal

A = absorption correction term

and $E\omega/I_o$ is called the integrated reflection.

The Lorentz factor L is concerned with the time required for a reciprocal lattice point to pass through the sphere of reflection. It varies with the geometries of different

experimental methods. For diffractometer data collected by the θ-2θ scan technique, it is given by

$$L = \frac{1}{\sin 2\theta} \tag{5}$$

The term p arises from a reduction of the scattered intensity due to polarization effects of electromagnetic radiation upon reflection and depends on the angle θ. If the incident beam is unpolarized, it is given by

$$p = \frac{1+\cos^2 2\theta}{2} \tag{6}$$

The absorption term A is the most difficult to calculate exactly as it requires a precise description of the crytal shape. The treatment of this problem in this work has been described in section 2.2.

Assuming the measured intensity* I_{obs} to be proportional to E_{ω} one can write

$$|F| = \sqrt{\frac{K\, I_{obs} A}{L p}} = |F_{obs}| \tag{7}$$

where K is the constant which reduces equation (4) to equation (7), and is known as the scale factor. Since the exact value of K is unimportant unless absolute magnitudes of the $|F|$'s are required, it has been omitted from the data reduction calculations. The $|F|$'s derived from the I_{obs} are

---

* Note the word "intensity" has been loosely used since it does not have the proper dimension for intensity, namely energy $cm^{-2}sec^{-1}$.

then $|F_{relative}|$'s (abbreviated as $|F_{rel}|$'s) defined as

$$|F_{rel}| = k' |F_{obs}| = \sqrt{I_{obs} A/Lp} \qquad (8)$$

A theoretical calculation of k' (=$1/\sqrt{K}$) is possible by means of the Wilson Plot[21a].

A reflexion was considered as observed if its intensity was $x\sigma$ times above the background (x was chosen as 1.8,2.0,2.5, and 2.0; $\sigma=\sqrt{N_c}$ where N_c is the scan+total normalized background counts). The "unobserved" reflexions were not included in the refinement. The computer program used was the NRCC Data Reduction program (by Ahmed and Pippy) with local modifications.

3.2 Solution of the Phase Problem

3.2.1 The Phase Problem

The structure factor F defined by (1) has both amplitude and phase. However, measurement of intensity will only furnish direct information of the amplitude of F (7) while its phase remains unknown. This is the well-known Phase Problem in x-ray diffraction. To recover the phases, two approaches have been used: the Direct Methods and the Patterson function.

3.2.2 Direct Methods

In Direct Methods, one tries to obtain an adequate set of phases to start with by considering the intensities themselves. Earlier studies, for example those by Sayre[21b], had lead to some useful relationships, which were later exploited by other workers, notably Hauptman and Karle.[22]

A number of relationships have been developed but the most powerful and widely used is the Σ_2 principle:

$$\text{sign}(E_h) \simeq \text{sign}\left(\sum_{k_r} E_k E_{h-k}\right) \qquad (9)$$

for centrosymmetric structures, and

$$\varphi_h \simeq \langle \varphi_k + \varphi_{h-k} \rangle_{k_r} \qquad (10)$$

for noncentrosymmetric structures. E_h is the normalized structure factor and φ_h is the phase of the structure factor of the reflexion h. The symbol $\simeq$ means "is probably equal to"; k_r implies that k ranges only over high $|E|$ reflexions. (10) is also written in the form known as the Tangent formula:

$$\tan \varphi_h = \frac{\sum |E_k E_{h-k}| \sin(\varphi_k + \varphi_{h-k})}{\sum |E_k E_{h-k}| \cos(\varphi_k + \varphi_{h-k})} \qquad (11)$$

The probability that the Σ_2 relationship is true, according to Woolfson and Cochran[23], is equal to

$$P \approx \tfrac{1}{2} + \tfrac{1}{2} \tanh\left\{\sigma_3 \sigma_2^{-3/2} |E_h E_k E_{h-k}|\right\} \qquad (12)$$

where $\sigma_3 = \sum_i Z_i^{\,3}$ and $\sigma_2 = \sum_i Z_i^{\,2}$, summation being over the unit cell and Z_i being the atomic number of atom i.

Both structures (I) and (III) were solved by Direct Methods, the former by the Symbolic Addition Procedure[24] (SAP) and the latter by the Tangent Refinement Program[25] (TRP). Both programs were obtained from NRCC (Ahmed&Hall;Hall&Huber). While these procedures are based on the Σ_2 principle, they

differ in the operations which extract the phases from the data. In the centrosymmetric case, the SAP gives tentative signs to the E's of the Σ_2 triplets when the product sum accumulated is higher than a test limit. Reflexions with acceptable tentative signs are then included in the list of signed reflexions and are used in turn. The test limit values are lowered successively (this ensures that only highly probable correct signs are included in the early stages of sign development) to generate more tentative signs. When the minimum test limit is reached and there are still reflexions with undetermined signs, a symbol is assigned to the reflexion that has the most triplets among the first ten highest E's. The whole process is repeated with the first test limit and so on. More symbols can be assigned if necessary (maximum of four). The program then seeks for consistent indication to determine the actual signs of the symbols and their products.

Symbolic addition procedures are suitable for centrosymmetric space groups but unsuitable for noncentrosymmetric ones due to the unrestricted nature of the phases. The TRP is written particularly for the noncentrosymmetric space groups though it is also applicable to the centrosymmetric cases. The TRP,in solving noncentrosymmetric structures,

has the advantage of refining the phases while the phase development continues. Ten cycles of phase extension and refinement are allowed, each with its own $|E|_{threshold}$ (the values decrease from cycles one to ten).

The allowable triplets with E values above the current threshold are scanned five times for use in (11). A principal test for reliability is given by the R_{karle} index defined as

$$R_{karle} = \frac{\sum \left| |E_h|_{obs} - |E_h|_{cal} \right|}{\sum |E_h|_{obs}} \qquad (13)$$

$|E_h|_{obs}$ is obtained from intensity data whereas $|E_h|_{cal}$ is obtained from the Tangent formula (11). A low R_{karle} may indicate a basically correct set of phases. An acceptance limit is specified for each cycle so that any reflexion with $|E|_{cal}$ below the limit is considered unreliable and rejected from the subsequent iteration.

The choice of origin reflexions, apart from satisfying the parity group requirements,should be exercised with care as they will initiate phase assignment and may therefore affect the phase development. If possible, these reflexions should interact among themselves, involve a relatively large number of triplets (especially with other large E values) and be among the largest E's. When additional phases are assigned to initiate the process, specially with TRP, they should also meet the same requirements.

While the TRP is definitely superior to symbolic addition procedures as far as noncentrosymmetric space

groups are concerned (the SAP program mentioned is generally not applicable to noncentrosymmetric space groups), it is hardly so in the centrosymmetric cases. There, while the SAP will in most cases give the answers in one run, leaving the worker to ponder over the symbols, the TRP may require 2^n runs if n additional reflexions are included to initiate phase assignment. In other words, the multiple solution case of the SAP can be viewed as slightly more elegant and economical than the single solution case of the TRP .

Another relationship which is implied by the Σ_2 principle is the Σ_1 relationship:

$$\text{sign } E_{2h} = \text{sign} \sum E_h E_h \qquad (14)$$

It should be noted that when the E's are sufficiently large E_{2h} will probably be positive regardless of the sign of E_h. This was used when part of the procedure was done manually in the solution of (I) as described in section 3.6.1.

It has been pointed out by Dewar[26] that the $\langle E^2 \rangle$'s of each parity group can be renormalized to 1 after intensity statistics calculation. This point is immaterial in cases where the E distribution in various parity groups approaches uniformity, but becomes crucial where this is not so. In the solution of (I), four parity groups had generally weak E's which were consequently undetermined by the SAP . Twenty-nine among the strongest of these were signed manually, which were proved later to be correct, although the small values of the E's relative to those of the strong subgroup led to a low probability of

certainty (12) when the E's were not normalized in the respective parity groups.

3.2.3 The Patterson Function

The Patterson function of an electron-density distribution

$$\rho(x,y,z) = \frac{1}{V} \sum_h \sum_k \sum_l F_{hkl} \exp\left[-2\pi i(hx + ky + lz)\right] \quad (15)$$

is defined[27] to be

$$P(u,v,w) = \int_0^1 \int_0^1 \int_0^1 \rho(x,y,z)\, \rho(x+u, y+v, z+w)\, V\, dx\, dy\, dz \quad (16)$$

or represented by the Fourier Series

$$P(u,v,w) = \frac{1}{V} \sum_h \sum_k \sum_l |F_{hkl}|^2 \exp\left[2\pi i(hu + kv + lw)\right]. \quad (17)$$

The physical significance of (16) is that P(u,v,w) is non-zero only for values of (u,v,w) that represent electron density overlap. For a set of N atoms, the Patterson function contains N^2 peaks, N of these coincide to form the origin peak. One half of the remaining (i.e. N(N-1)/2) peaks are related to the other half by a centre of symmetry. The weight of a Patterson peak is proportional to the product of the atomic numbers of the two atoms involved. Peaks generated by the heavy atoms are therefore prominent in the map. In general, a set of chemically reasonable atomic coordinates can be worked out to fit the major features of the Patterson map. Because of the nature of convoluted function, the Patterson peaks are considerably broader than the atomic peaks. If the number of

heavy atoms is small(for example, it is four in structures (II) and (IV)) in the asymmetric unit, accidental coincidence of the peaks should not be expected to be too serious.

The symmetry of the crystal usually provides useful information concentrated in certain planes or lines of the three-dimensional Patterson function known as the Harker sections or lines. (Harker sections are more useful than Harker lines because of less overlap of peaks.) For instance a crystal belonging to a space group containing a two-fold b axis will give a Patterson peak with weight proportional to Z_i^2 at the plane $(2x_i, 0, 2z_i)$ corresponding to every vector between symmetry-related atoms at (x_i, y_i, z_i) and $(x_i, -y_i, z_i)$. In the structure solution of (IV), the systematic absences were consistent with both $Pna2_1$ and Pnam space groups. The only Harker section derived from the former space group was at z=1/2 while the latter space group had additional Harker sections at y=1/2 and x=1/2. Since it was observed in the Patterson map that a concentration of peaks was found in the plane at z=1/2 only, the structure was assumed to belong to the space group $Pna2_1$.

3.3 Fourier Synthesis

Equation(15) gives the electron-density distribution in a Fouier series representation. The coefficients F's for the first Fourier electron density map can be obtained by two methods. Direct Methods yield a set of phased E's

which gives the phases of a corresponding set of F's whose amplitudes can be obtained from (8). This set of F's* can then serve as coefficients in (15). Although the summation is not over the entire hkl values measured, the electron density map will give initial atomic positions since the input F's are always large in their respective ranges of $\sin\theta/\lambda$. On the other hand, solution of the Patterson function gives a set of atomic coordinates from which approximate F_{cal}'s can be computed(1) assuming some temperature factors. Usually the phases of the F_{cal}'s and the amplitudes from the F_{rel}'s are used as input to (15). If the heavy atoms represent a high percentage of the scattering material, they should be sufficiently good to constitute an initial phasing model even though the summation of (1) is not over the entire contents of the unit cell if some positions of the light atoms are not recovered from the Patterson map.

If the quantities $\Delta F=F_{obs}-F_{cal}$, where F_{obs} takes the phase of the corresponding F_{cal}, are used as coefficients in the Fourier series instead, an electron density difference map is obtained. As suggested by the definition of ΔF, the map will reveal the difference between the true structure and the model used. It is therefore useful in locating light atoms, correcting misplaced atoms and detecting anisotropic thermal motion. Since ΔF depends on F_{cal} as well, a fairly good model should be obtained before the difference map can

* Since the series termination errors in an E map are more serious than those in a corresponding F map, it is expected to be more difficult in locating light atom positions in a heavy atom structure. However in a more equal-atom type structure, an E map will serve just as well.

be of substantial help. It should also be noted that when a F_{cal} is small, its phase cannot be treated as reliable.

The Fourier synthesis program used throughout this work was FORDAP written by Dr.A.Zalkin, University of California. It has options for computing the Patterson, electron density and difference maps.

3.4 Structure Refinement

3.4.1 Least-Squares Method

After a trial phasing model is obtained, refinement of the scale k′ between the observed and calculated structure factors, and positional as well as thermal parameters of the atoms is by full-matrix least-squares methods[28]. The quantity to be minimized is

$$D = \sum_{hkl} w_{hkl} \left(|F_{rel}| - k' |F_{cal}| \right)^2 \equiv \sum_{hkl} w_{hkl} \Delta^2 \qquad (18)$$

or alternatively

$$D_2 = \sum_{hkl} w_{hkl} \left(|F_{rel}|^2 - k'^2 |F_{cal}|^2 \right)^2 \qquad (19)$$

It has been pointed out that if the weights, w_{hkl}'s, represent the uncertainties of the terms of the summation in each case, both forms should lead to the same final results. In this work, (18) was used throughout. It should be noted that while the scale factor k' is a variable and ought to be applied to F_{cal} in a least-squares refinement, the reciprocal of k' is applied to F_{rel} in the printout of the structure factor tables so that the results are in

electrons.

The functional form of the structure factor is non-linear, therefore it has to be approximated by a truncated Taylor series. The refined values of the parameters from a cycle of least squares procedure are only better approximations to their best values than those before refinement. Calculation must therefore be repeated until the iterative process produces no significant change in the parameters.

3.4.2 The Weighting Scheme

The choice of weights in the least-squares refinement is very important as an improper choice can lead to erroneous results. In general there are two approaches[29]. The first is to set $w=1/\sigma^2(F)$ where $\sigma^2(F)$ is the variance of F obtained from the intensity counting statistics. The second is to construct a weighting scheme empirically which (i) eliminates trends of $\langle w\Delta^2 \rangle$ with respect to ranges of F_{rel}, $\sin\theta/\lambda$ etc., and (ii) adjusts the error of fit $[\Sigma w\Delta^2/m-n]^{\frac{1}{2}}$ to unity (m-n=number of observations-number of variables) so that the weights obtained are the best in the least-squares sense. Step (ii) is important to yield the 'correct' values for the standard errors. The two approaches differ in the sense that the first one is trying to achieve absolute weights while the second one searches for the best relative weights. In this work the second approach was followed.

The subroutine for the weighting scheme in the least-squares program BUCILS (based on UCILS, Northwestern University and University of California, Irvine, and modified at University of Canterbury, N.Z.) was changed so that with $w=1/\sigma$,

$$\begin{aligned} \sigma &= \sqrt{A'} && \text{for} \quad B < F_{obs} \leqslant C \\ \sigma &= \sqrt{A'}\,\frac{B'}{F_{obs}} && \text{for} \quad B \geqslant F_{obs} \\ \sigma &= \sqrt{\frac{A' F_{obs}}{C}} && \text{for} \quad C < F_{obs} \end{aligned} \tag{20}$$

3.4.3.Agreement Criterion

The agreement between the observed and calculated F's is shown by the R-factor defined as

$$R = \left(\sum |\Delta|\right) / \sum |F_{obs}| \tag{21}$$

and the weighted R_w-factor

$$R_w = \left[\left(\sum w|\Delta|^2\right) / \left(\sum w|F_{obs}|^2\right)\right]^{1/2} \tag{22}$$

Hamilton [30] considered the question of meaningful changes in the agreement when the model was altered. The ratio $R_w(1)/R_w(2)$ (or one may take $R(1)/R(2)$ as a close approximation), where (1) and (2) denote before and after the alteration of the model, can be compared with the appropriate value for those dimensions of test(the number of new variables introduced and the degrees of freedom) at a given

level of significance. This test has been applied to justify the introduction of new variables especially in the later stages of refinement of the four crystal structures.

3.4.4 Secondary Extinction

In (II) and (III), effects of secondary extinction[31] were observed near the final stages of refinement. Comparison of the low angle strong reflexions showed that the $|F_{cal}|$'s were consistently larger than the $|F_{rel}|$'s. An isotropic secondary extinction parameter E_c [32] was introduced in BUCILS so that the following expression is minimized:

$$D_E = \sum w \left(|F_{rel}| - \frac{k\,|F_{cal}|}{1 + E_c\, I_{obs}} \right)^2 \qquad (23)$$

3.5 Thermal Motion Correction for Bond Lengths

It has been pointed out[33] that the thermal motion in atoms has the effect of shortening the mean separations between the atoms. In some cases the error in using uncorrected values of bond lengths is so large that the least-squares estimated standard errors can give a misleading impression of the bond length precision.

If $\underline{w}_A$ and $\underline{w}_B$ are the projected instantaneous displacements of the two atoms A and B on the plane normal to their line of mean positions, then the value of $\overline{w_o^2}$, where $\underline{w}_o = \underline{w}_A - \underline{w}_B$ = relative displacement vector of A and B, can be expressed in terms of the mean components of displacements of each atom which are experimentally accessible. It can be shown that[34]

$$w_L^2 \leqslant \overline{w^2} \leqslant w_U^2 \qquad (24)$$

where $w_L^2 = [(\overline{w_B^2})^{\frac{1}{2}} - (\overline{w_A^2})^{\frac{1}{2}}]^2$

$$w_U^2 = [(\overline{w_B^2})^{\frac{1}{2}} + (\overline{w_A^2})^{\frac{1}{2}}]^2$$

and therefore

$$S_o + w_L^2/2S_o \leqslant \bar{S} \leqslant S_o + w_U^2/2S_o \qquad (25)$$

where S_o = uncorrected distance

S = true mean interatomic distance

Hence the upper and lower bounds can be placed on the mean separation of two atoms without any assumption as to the correlation of their motion. The lower bound corresponds to highly correlated parallel displacements of the two atoms and the upper bound to highly correlated antiparallel displacements.[34]

Two models for the evaluation of S have been proposed:

(i) the "riding" atom - when B is riding on A,

$$\overline{w^2} = \overline{w_B^2} - \overline{w_A^2} \qquad (26)$$

and

$$\bar{S} = S_o + (\overline{w_A^2} - \overline{w_B^2})/2S_o \quad , \qquad (27)$$

this proves to be a useful approximation when B is strongly bonded to A and to few other atoms;

(ii) the independent atom model - when A and B are completely non-interacting,

$$\bar{S} = S_o + (\overline{w_A^2} + \overline{w_B^2})/2S_o \quad , \qquad (28)$$

this provides an approximation for non-bonded atoms in a molecular crystal.

Bond lengths and angles with standard errors estimated from the least-squares refinement and from the errors in cell-dimension measurements were calculated using the program ORFFE(Busing and Levy). Functions to calculate the various r.m.s. displacements of the atoms, and correction of bond lengths from the riding and independent models were available.

Another program to correct thermal motion effects on bond lengths was the Rigid Body Program (Schomaker and Trueblood[35]). The four heavy atoms in (IV) had been considered for such correction but the thermal ellipsoids suggested the model was not appropriate in this case.

Furthermore, a program was written during the course of this work to compute the U_{ij}'s from the B_{ij}'s of the atoms and the lower and upper bound limits of bond lengths according to (25). This is described in the Appendix.

3.6 Solution and Refinement of Each Structure

3.6.1 Structure Analysis of $(C_5H_5)_2Cr_2(NO)_3(NH_2)$

Among the 903 independent reflexions measured, 511 were above 1.8σ and were considered as observed. An examination of the intensity data revealed that they could be divided into two parts: the $h+k$ even reflexions were in general much more intense than the $h+k$ odd.

Applying the SAP program to the data with origin determining reflexions 1 1 1 (E=2.81), 6 1 5 (E=2.71) and 6 2 3 (E=2.64) (E_{max} =3.90, E_{min} =1.2) yielded 236 signed reflexions which all belonged to the $h+k=2n$ class. A Fourier map derived gave an approximate structure. However, in spite of the good agreement(R= 0.21) and chemical reasonableness, the pseudo C-centred symmetry could not be destroyed. It was also noted that amongst the $hk0$ zone only 6 reflexions were observed for $h+k=2n+1$ and were weak in intensity. This strongly indicated an approximate n-glide plane normal to c in addition to the general C-centring.

The phases of the data based on the significant chromium atom contributions could be taken with confidence and the Sayre relationship was applied to the remaining unknown phases. The normalization of the E's in each parity group (see Section 3.2.1) would give an equivalent result. Among the $h+k$ odd data, 39 relatively stronger reflexions

were selected. As many as 128 triplets were found amongst themselves and the signed reflexions of high E's. Sayre relationships were first constructed within each parity group and later extended to inter-parity-groups. It was found that two further subgroups existed (eoe and oeo; oee and eoo) with a small number of relationships between them. It can be seen from Table II that twice as many triplets were found for the first subgroup as the second. Among the six symbols employed, four could be signed with confidence and yielded 29 phases all of which proved subsequently to be correct. An electron density Fourier map of the total 256 signed F_{rel} successfully indicated the distortion of the structure from the C-centred lattice.

The two independent chromium atoms occupied special positions at y=0.25 but had very similar x coordinates (they were found to be on either side of x=-0.25 and this was responsible for the pseudo-C-centring). The terminal nitrosyl groups were also located at special positions at y=0.25. The bridging NO group was observed as a broad peak, being disordered with the NH_2 group with respect to the crystallographic symmetry plane at y=0.25. Areas of the cyclopentadiene rings consisted of broad and non-spherical peaks, the best description being two disordered orientations of equal occupancy for each ring.

Refinement by full-matrix least-squares (unit weights)

TABLE II. $\underline{h}+\underline{k}$ odd Reflexions

	subgroup 1 eoe oeo	subgroup 2 oee eoo
range of F_{rel}	7-14	7-26
range of E	0.177-0.740	0.229-0.850
no. of reflexions selected	22	17
no. of reflexions signed	17	12
no. of triplets	82	39
no. of triplets between subgroups	16	

converged slowly because of a large number of severe interactions (refer to Table III) amongst the coordinate parameters since the coordinates of one 'half' of the molecule were approximately related to those of the other half by a twofold axis (positions x,y,z and $-\frac{1}{2}$-x,y,-z were in general nearly equivalent). The pseudo-C centring found at the time of structure solution also provided a warning of these interactions, in an equivalent manner to the coincidences in the Patterson function mentioned by Geller[36].

A three-dimensional electron density difference map at R=0.12 revealed that the largest features were associated with the two chromium and terminal nitrosyl oxygen atoms. While the least-squares refinement gave the x-coordinates for the chromium atoms as -0.264 and -0.220, the electron density map suggested values of -0.27 and -0.24 instead (final refined values being -0.2775 and -0.2334). Apparently the least-squares method had refined to a pseudo-minimum situation because the initial parameter chosen required the path of refinement to cross from one side of the pseudo-equivalent position (x,y,z; $-\frac{1}{2}$-x,y,-z) to the other. The new positions improved considerably the consistency of the distances between the chromium and light atoms.

After correction of the chromium atomic coordinates the terminal nitrosyl oxygen atoms were allowed anisotropic

TABLE III

Correlation Coefficients (> .4) for Interacting Pairs of Coordinate Parameters of (I)

Cr	1	x	Cr	2	x	.46
		z			z	.42
C	1	x	C	03	x	.45
		z			z	.55
C	3	x	C	01	x	.44
		z			z	.43
		y	C	6	y	.44
C	4	z	C	06	z	.43
C	5	x	C	06	x	.40
C	6	x	C	04	x	.42
C	01	x	C	04	x	.45
C	03	y	C	06	y	.69
		z			z	.43
N	1	x	N	2	x	.40

motion. Refinement proceeded and a final R factor of 0.069 was obtained. It was found useful, because of the large interactions, to refine non-interacting parameters in various combinations to eliminate oscillations before the final two cycles of full-matrix least-squares refinement (Partial shifts would probably have accomplished the same result). A final electron density difference map showed no feature greater than 0.5e $\mathring{A}^{-3}$.

In this centrosymmetric model of the structure, the NO and NH_2 bridges were disordered and could not be distinguished. The noncentrosymmetric model had not been pursued because in such a case the number of severe interactions would be expected to increase correspondingly. Furthermore it is possible that the cyclopentadiene rings are disordered even in the noncentrosymmetric case. The ratio of observations to variables will decrease to a rather low value (see N/V in abstract). Information of chemical interest thus obtained will not be expected to differ significantly from what is already known about the structure from the centrosymmetric model.

The final coordinates and temperature parameters are listed in Table IV, interatomic distances and angles in Table V, least-squares planes in Table VI and the structure factors in Table VII, the molecular diagram and the packing of the molecules in the unit cell are shown in Figures 1 and 2.

TABLE IV

Atomic Coordinates and Thermal Parameters of(I)

	x	y	z	($Å^2$)
Cr 1	-.2774(4)	.2500	.0774(2)	3.24(8)
Cr 2	-.2344(4)	.2500	-.0728(2)	3.04(8)
O 1	-.6255(23)	.2500	.1073(17)	*
O 2	.1286(20)	.2500	-.0766(16)	*
O 3	-.3144(22)	.5172(23)	-.0011(13)	4.8(4)
N 1	-.4818(28)	.2500	.0892(11)	5.1(4)
N 2	-.0232(28)	.2500	.0698(12)	5.6(5)
N 3	-.2712(17)	.4019(11)	.0014(8)	4.2(2)
C 1	-.2060(82)	.2500	.2052(32)	5.6(14)
C 2	-.1610(37)	.3896(35)	.1687(16)	2.3(5)
C 3	-.0188(25)	.3340(27)	.1183(11)	1.1(3)
C 01	-.0090(103)	.2500	.1142(42)	7.9(19)
C 02	-.0978(52)	.3581(48)	.1503(22)	4.4(10)
C 03	-.2423(48)	.3149(61)	.1963(21)	4.0(8)
C 4	-.2281(66)	.2500	-.1988(27)	3.7(10)
C 5	-.3313(55)	.3581(46)	-.1767(22)	4.2(9)
C 6	-.4674(43)	.3259(42)	-.1373 (18)	2.7(7)
C 04	-.4852(49)	.2500	-.1277(22)	2.2(8)
C 05	-.3916(59)	.3878(54)	-.1546(25)	6.3(11)
C 06	-.2552(54)	.3356(60)	-.1907(22)	4.5(9)

	U_{11}†	U_{22}	U_{33}	U_{12}	U_{13}	U_{23}
O 1	38(5)	36(6)	12(5)	0	06(14)	0
O 2	39(5)	21(3)	12(4)	0	13(13)	0

*Anisotropic thermal parameters for O 1 and O 2.

†These values were obtained from $\beta_{ij} = 2\pi^2 b_i b_j U_{ij}$ where β_{ij} appear as a temperature effect through exp $[- (\beta_{11} h^2 + 2\beta_{12} hk + \ldots)]$ in the structure factor expression and b_i's are the reciprocal lattice vectors. The U_{ij}'s are in $10^3 Å^2$.

TABLE V. Interatomic Distances and Angles for (I)

(a) Bonded distances (Å)

	Cr(1)-Cr(2)	2.650 (4)
	Cr(1)-N(1)	1.637 (23)
	Cr(2)-N(2)	1.672 (23)
	Cr(1)-N(3)	1.936 (12)
	Cr(2)-N(3)	1.936 (12)
Average	Cr—C	2.24 (5)
	N(1)-O(1)	1.185 (27)
	N(2)-O(2)	1.212 (25)
	N(3)-O(3)	1.121 (22)
Average	C—C	1.43 (11)

(b) Angles (°)

Cr(1)-N(1)-O(1)	171.7 (2.4)
Cr(2)-N(2)-O(2)	172.6 (2.5)
Cr(1)-N(3)-O(3)	135.1 (1.7)
Cr(2)-N(3)-O(3)	135.4 (1.7)
N(1)-Cr(1)-N(3)	96.4 (0.7)
N(2)-Cr(2)-N(3)	97.7 (0.7)
N(3)-Cr(1)-N(3)	93.1 (0.8)
Cr(1)-N(3)-Cr(2)	86.4 (0.5)
N(3)-Cr(2)-N(3)	93.1 (0.8)

(c) Intermolecular contacts (<3.25 Å)

O(1)	O(3)	2.88 Å	1*
	C(3)	3.05	2
	C(01)	3.23	2
O(2)	O(3)	2.94	3
	C(04)	3.20	4
O(3)	O(3)	2.97	1
	N(1)	3.10	1

* key for symmetry relationship:

1	-1-x	1-y	-z
2	-1+x	y	z
3	-x	1-y	-z
4	1+x	y	z

TABLE VI. Deviations for Mean Planes of (I)

Equations of Planes*	Atoms in Plane	Atom out of Plane	Deviation(Å)
(-0.7884)x + (0.0000)y + (0.6152)-(-1.5391) = 0	C 2, C 2' C 3, C 3'	C 1	-.28(6)
(-0.8188)x + (0.0000)y + (-0.5741)z -(-1.7059) = 0	C 02, C 02' C 03, C 03'	C 01	-.11(8)
(-0.8435)z + (0.0000)y + (-0.5371)z - (4.0206) = 0	C 5, C 5' C 6, C 6'	C 4	-.11(5)
(0.8643)x + (0.0000)y + (-0.5030)z - (3.9024) = 0	C 05, C 05' C 06, C 06'	C 04	-.03(4)
(-0.1317)x + (-0.0897)y + (-0.9872)z - (1.7916)= 0	Cr 1, Cr 2, N 3		
(-0.1317)x + (+0.0897)y + (-0.9872)z - (2.2066) = 0	Cr 1, Cr 2, N 3'		

*The coordinates are referred to the orthogonal axes of the unit cell in Å

TABLE VII

Measured and Calculated Structure Factors of (I)

scale = $10 \times F_{absolute}$

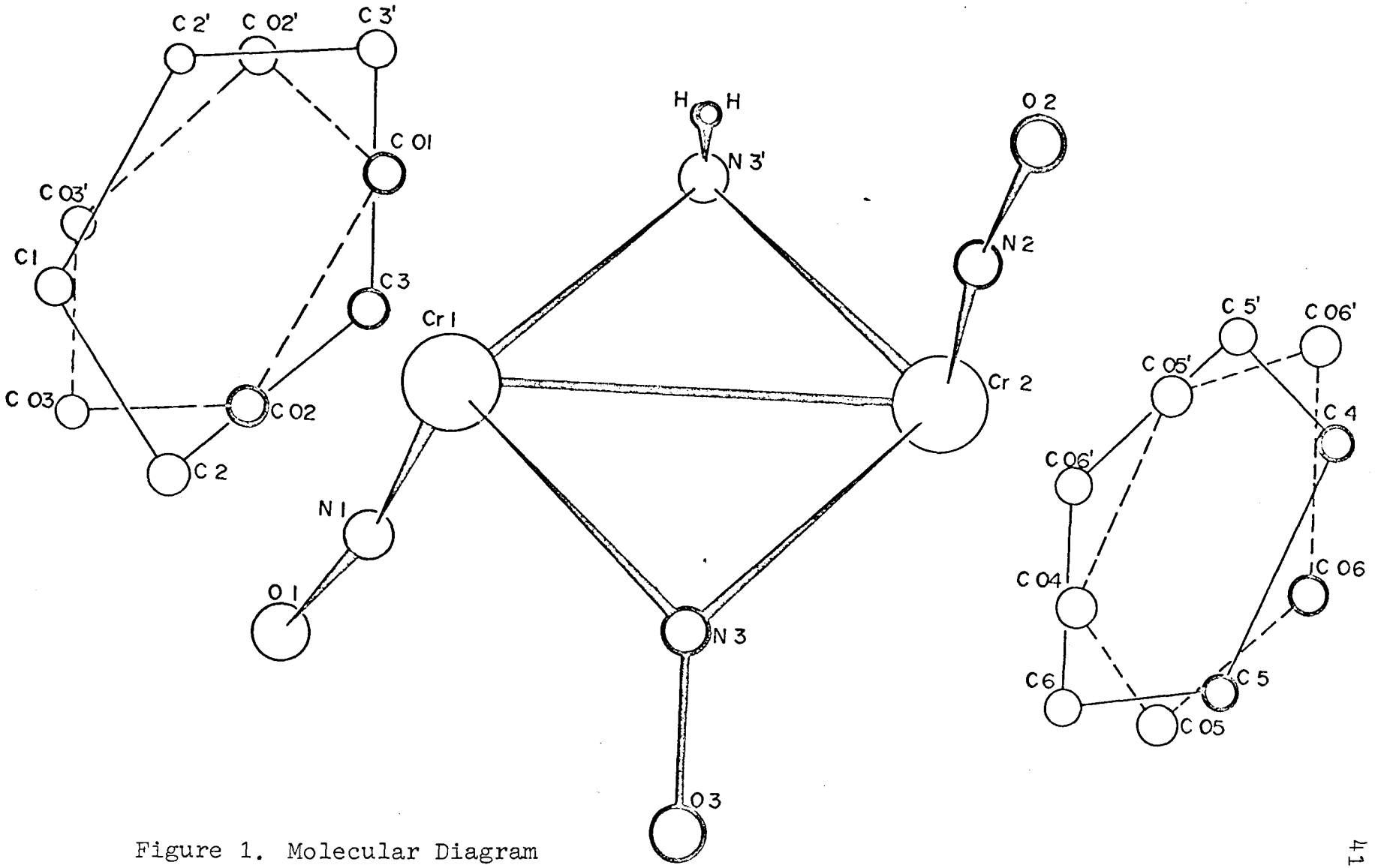

Figure 1. Molecular Diagram
of $(C_5H_5)_2Cr_2(NO)_3(NH_2)$

Figure 2

Packing Diagrams of $(C_5H_5)_2Cr_2(NO)_3(NH_2)$

of The Unit Cell

(a)projected down a

(b)projected down b

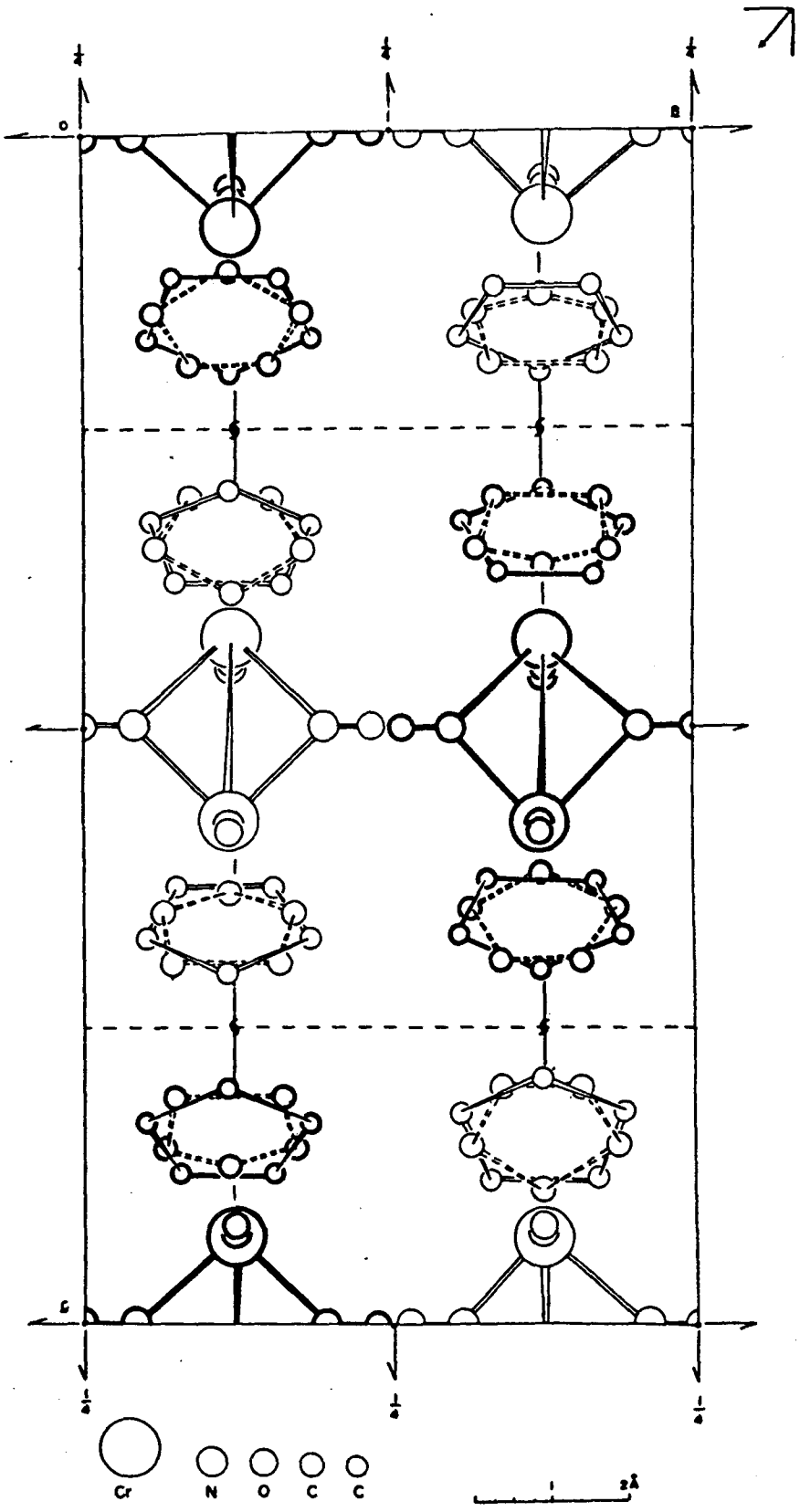

Figure 2(a)

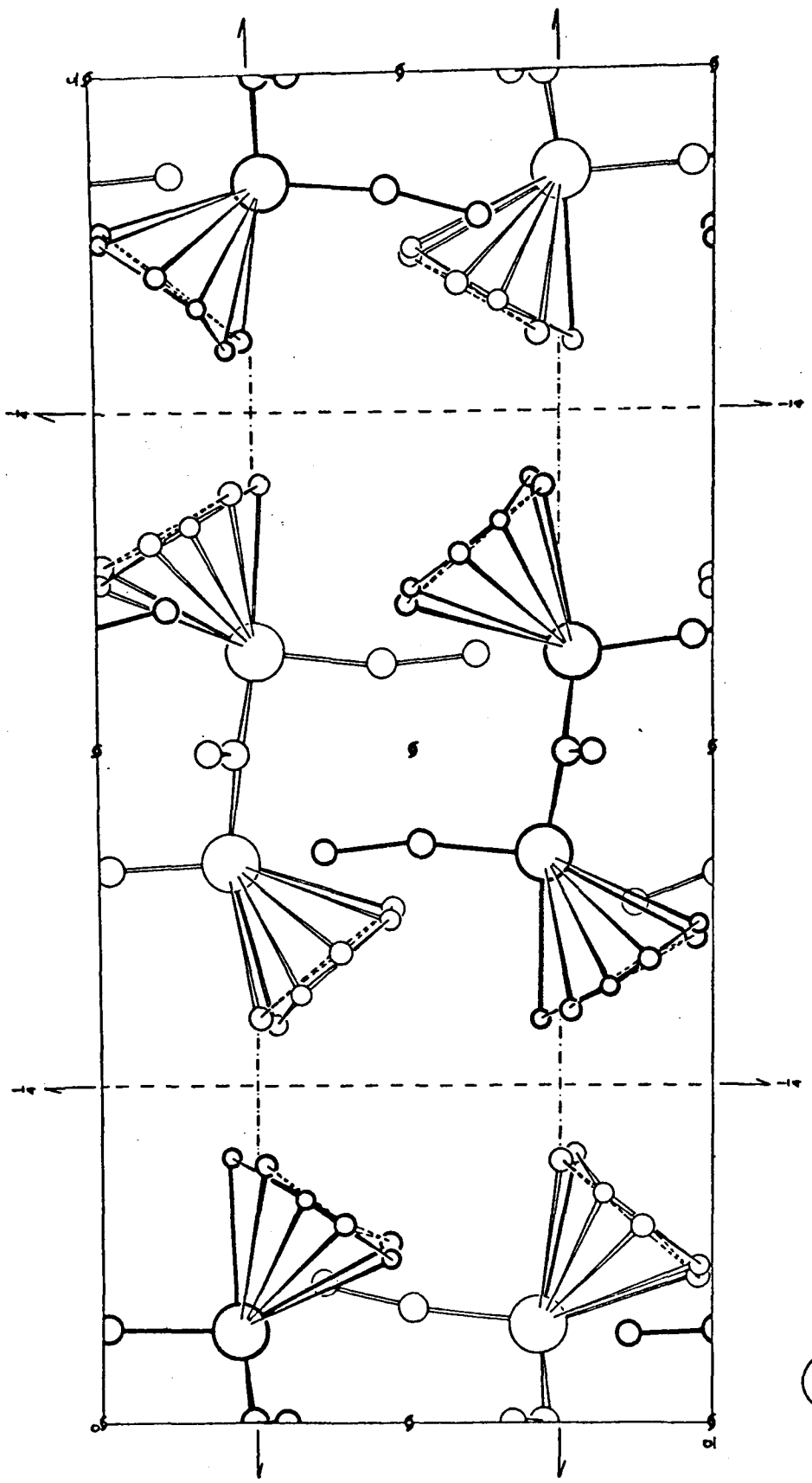

Figure 2(b)

3.6.2 Structure analysis of $KIO_3.HIO_3$

Of the 1644 independent intensities measured for $KIO_3.HIO_3$, 1392 were above 2σ and were considered as observed reflexions. Density and space group requirements suggested that there were eight formula units per unit cell. The phase problem was solved by Patterson Synthesis which gave the positions of the four iodine atoms. A three dimensional electron-density map (at R=0.30) showed two potassium atomic positions. Two cycles of least-squares refinement on these six atoms gave an R of 0.20. An electron density difference map revealed all twelve oxygen atoms around the iodine atoms. One cycle of least-square refinement of all the non-hydrogen atoms with isotropic temperature factors improved the agreement to 0.132.

Examination of the $|F_{rel}|$ and $|F_{obs}|$ at this stage showed that the experimental absorption curve was too severe and it was modified to be less so. The R factor improved spectacularly to 0.071. Two cycles of refinement on isotropic thermal and coordinate parameters led to an R of 0.058. At this point, effects due to secondary extinction were observed (section 3.4.4) and the appropriate parameter E_c was introduced (the final value for E_c being $8.4(5) \times 10^{-7}$). The R factor dropped to 0.054 with all isotropic temperature factors. An electron density difference map

showed anisotropic thermal motion about the iodine atoms allowing for which brought the R to 0.050 with negligible further shift. Until completion of refinement w=1 had been used throughout; $< w\Delta^2 >$ was trendless as a function of sin θ/λ, F_{rel} and other factors. For the final cycle, w was given a constant value (.1307) such that the error of fit was 1.0 to give the best possible standard errors in the atomic parameters. An electron density difference map computed after the refinement was complete showed no positive peaks greater than 0.7e/Å^3 (the largest peak being at 0.8Å from O(12)), although a negative trough of -1.2 e/Å^3 was found at 1.4Å from I(3).

The molecular packing diagram is shown in Figure 3. The final coordinates and temperature parameters are listed in Table (VIII), the interatomic distances and angles in Table (IX) and the structure factors in Table (X).

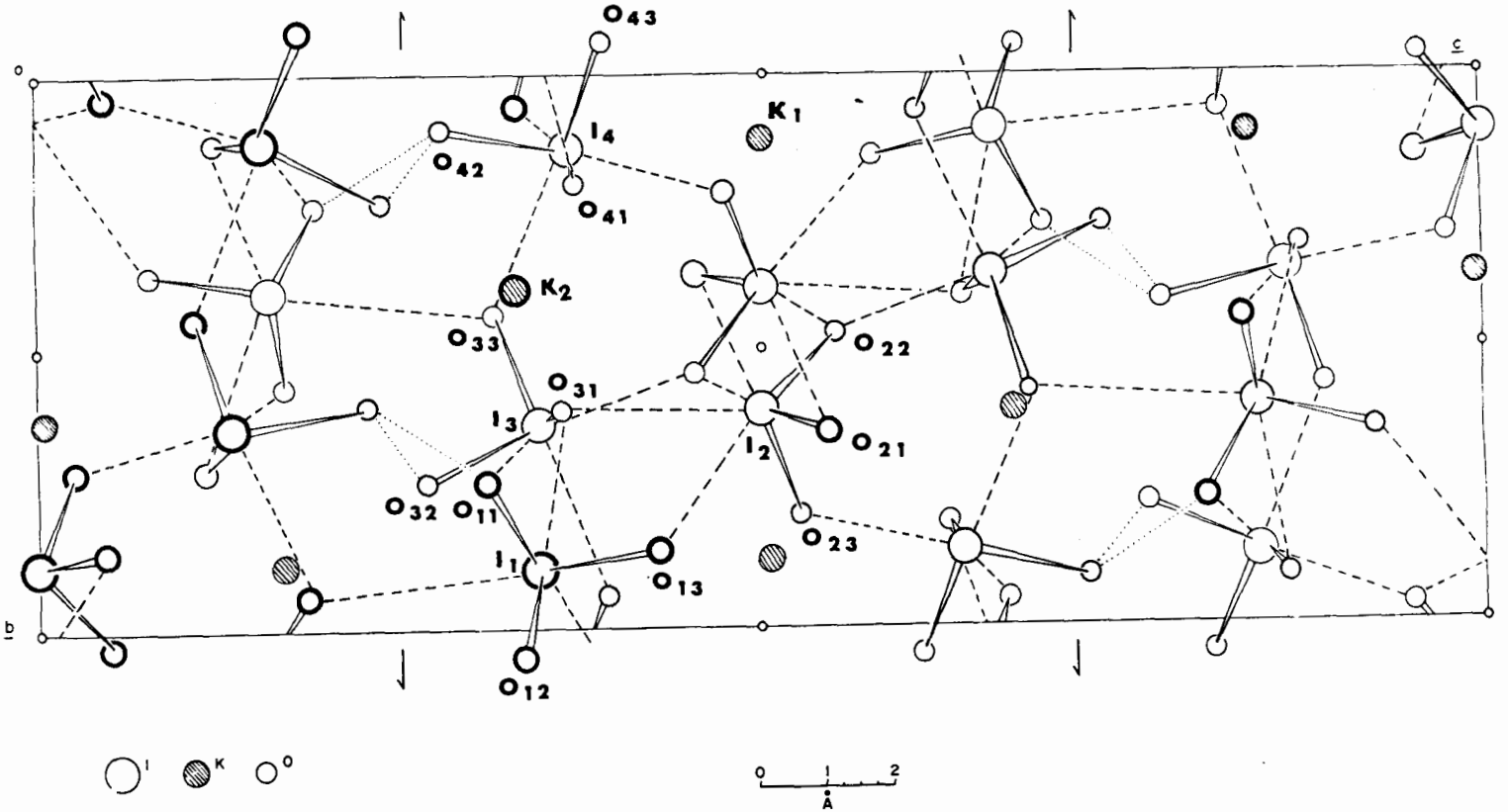

FIG. 3. Crystal structure of $KIO_3.HIO_3$ viewed down the a^* axis. (Dotted lines indicate hydrogen bonds, dashed lines weak I---O interactions.)

TABLE VIII

Atomic Parameters for $KIO_3.HIO_3$

Coordinates

Atom	X	Y	Z	B(Å)²
I(1)	0.1688(2)	0.1045(2)	0.6573(1)	*
I(2)	0.2314(2)	0.3873(2)	0.4998(1)	*
I(3)	0.6678(2)	0.3679(2)	0.6563(1)	*
I(4)	0.6524(2)	0.8605(2)	0.6359(1)	*
K(1)	0.2498(7)	0.8765(7)	0.5034(2)	1.60(9)
K(2)	0.1444(7)	0.6136(7)	0.6715(2)	1.79(9)
O(11)	0.0531(21)	0.2675(18)	0.6925(7)	1.4†
O(12)	0.0150(22)	0.9416(20)	0.6691(7)	1.9
O(13)	0.0986(22)	0.1429(20)	0.5758(7)	2.0
O(21)	0.0014(21)	0.3560(19)	0.4534(7)	1.6
O(22)	0.3192(22)	0.5407(20)	0.4524(7)	1.8
O(23)	0.3501(22)	0.2093(19)	0.4744(7)	1.6
O(31)	0.4159(23)	0.3994(22)	0.6383(8)	2.2
O(32)	0.6475(22)	0.2708(20)	0.7347(7)	1.9
O(33)	0.7410(23)	0.5658(20)	0.6851(8)	2.1
O(41)	0.4045(21)	0.8058(19)	0.6276(7)	1.4
O(42)	0.6645(20)	0.9027(19)	0.7243(7)	1.4
O(43)	0.6229(22)	0.0612(20)	0.6086(7)	1.9

Atom	U_{11}*	U_{22}	U_{33}	U_{12}	U_{13}	U_{23}
I(1)	96(7)	164(8)	173(8)	-41(7)	11(6)	-15(7)
I(2)	135(8)	157(8)	109(8)	- 7(7)	19(6)	- 5(7)
I(3)	112(8)	128(8)	173(8)	0(6)	17(6)	5(7)
I(4)	101(8)	120(8)	173(8)	2(6)	25(6)	19(7)

* Anisotropic thermal parameter used for Iodine atoms $(Å)^2 \times 10^4$

† Standard error of the B's of the oxygen atoms are less than $0.3A^2$

TABLE IX. Interatomic Distances and Angles of $KIO_3.HIO_3$

(A) I-O bonded distances

Predicted Formal Bond Order	Contacts	Observed bond length Å	Average length Å *
2	I(3)-O(31)	1.778(17)	1.776(17)
	I(3)-O(33)	1.791(17)	
	I(4)-O(41)	1.784(15)	
	I(4)-O(43)	1.753(17)	
$1\frac{2}{3}$	I(2)-O(21)	1.818(15)	1.796(21)
	I(2)-O(22)	1.792(16)	
	I(2)-O(23)	1.807(15)	
	I(1)-O(11)	1.793(15)	
	I(1)-O(12)	1.759(16)	
	I(1)-O(13)	1.808(16)	
1	I(3)-O(32)	1.911(17)	1.932
	I(4)-O(42)	1.952(15)	

* The standard errors in the average values are estimated from the internal consistency and show no significant difference between bonds of predicted orders $1\frac{2}{3}$ and 2.

Table (IX) continued

(B) Interionic Contacts (I-O and K-O < 3.5Å)

Type of Contact		Distance*	Symmetry Relationship†	Average Distance
I(1)	O(31)	3.04	1	
	O(41)	3.08	1a	3.18
	O(33)	3.43	3	
I(2)	O(13)	2.84	1	
	O(21)'	2.93	2a	
	O(31)	3.12	1	3.03
	O(22)'	3.24	2	
I(3)	O(22)	2.50	2	
	O(43)	2.72	1	2.69
	O(11)	2.84	1b	
I(4)	O(23)	2.47	2	
	O(12)	2.64	1b	2.60
	O(33)	2.68	1	
K(1)	O(13)	2.80	2a	
	O(13)	2.98	1c	
	O(21)	2.83	2a	2.88
	O(22)	3.04	1	
	O(23)	2.87	2	
	O(23)	2.91	1c	
	O(41)	2.84	1	
	O(43)	2.77	2	
K(2)	O(11)	2.96	1	
	O(12)	2.84	1	
	O(21)	2.78	2a	
	O(31)	2.76	1	2.83
	O(32)	2.68	3a	
	O(33)	2.92	1d	
	O(41)	2.69	1	
	O(42)	3.02	3a	

* Standard errors in these distances are all less than ± 0.02Å

† Key for symmetry relationship

1) x,y,z
1a) x,y-1,z
1b) x+1, y,z
1c) x, y+1, z
1d) x-1, y, z

2) 1-x, 1-y, 1-z
2a) 1-x, y-½, 3/2-z
3) 1-x, y-½, 3/2-z
3a) 1-x, y+½, 3/2-z
4) 1-x, -y, 1-z

Table IX continued

(C) Angles (°) around Iodine atoms

(a) both I-O<2.00Å

(b) 2.40A<both I-O<3.5Å

(c) One I-O<2.00Å
2.40A<One I-O<3.5Å

	Distorted Octahedra I(1)		I(3)		I(4)		Distorted-Capped Octahedron I(2)	
(a)	O(11),O(12)	100.4(7)	O(31),O(32)	93.6(8)	O(41),O(42)	93.6(7)	O(21),O(22)	97.7(7)
	O(12),O(13)	100.7(8)	O(32),O(33)	96.7(8)	O(42),O(43)	99.0(7)	O(22),O(23)	100.3(7)
	O(13),O(11)	102.3(8)	O(33),O(31)	100.0(8)	O(43),O(41)	97.7(8)	O(23),O(21)	97.7(7)
(b)	O(31),O(41)	105.7	O(22),O(43)	86.1	O(12),O(33)	87.4	O(21)¦O(22)'	108.5
	O(41),O(33)	96.3	O(22),O(11)	101.0	O(23),O(12)	101.6	O(21)¦O(13)'	93.5
	O(31),O(33)	100.6	O(11),O(43)	83.9	O(33),O(23)	98.6	O(13),O(22)'	109.0
							O(21)¦O(31)	79.3
							O(22)¦O(31)	55.1
							O(13),O(31)	65.3
(c)	O(11),O(41)	167.0	O(31),O(11)	170.7	O(41),O(12)	170.0	O(21),O(22)'	165.1
	O(12),O(31)	176.7	O(32),O(22)	172.4	O(42),O(23)	176.3	O(22),O(13)	179.0
	O(13),O(33)	172.9	O(33),O(43)	169.7	O(43),O(33)	172.7	O(23),O(21)'	172.1
	O(11),O(31)	76.6	O(31),O(22)	85.0	O(41),O(23)	88.2	O(21),O(13)	83.2
	O(11),O(33)	70.8	O(31),O(43)	89.4	O(41),O(33)	89.0	O(21),O(21)'	78.4
	O(12),O(33)	79.3	O(32),O(11)	79.5	O(42),O(33)	77.7	O(22),O(22)'	70.0
	O(12),O(41)	77.6	O(32),O(43)	86.5	O(42),O(12)	77.1	O(22),O(21)'	87.0
	O(13),O(31)	78.9	O(33),O(22)	90.9	O(43),O(12)	85.5	O(23),O(22)'	77.0
	O(13),O(41)	90.7	O(33),O(11)	87.0	O(43),O(23)	84.3	O(23),O(13)	79.2
							O(31),O(21)'	139.8
							O(31),O(22)	114.0
							O(31),O(23)	100.1

Table IX continued

(D)O-O Interionic distances(< 3.00Å) and selected angles (°)

Type	Distance(Å) or angle(°)	Symmetry ‡ relationship
O(22)-O(31)	2.94*	1
O(23)-O(43)	2.89	4
O(12)-O(42)	2.91	1d
O(33)-O(42)	2.97	1
O(11)-O(42)	2.73†	4
O(42)-O(32)	2.71†	3a
I(3)-O(32)-O(42)	107.1(8)	
I(4)-O(42)-O(32)	109.5(7)	
I(4)-O(42)-O(11)	120.9(8)	
I(1)-O(11)-O(42)	104.9(7)	
O(32)-O(42)-O(11)	99.5(7)	

* standard deviation in these distances all less than ± 0.03Å

† hydrogen bonded O...HO distances

‡ as in table B

Table X

Measured and Calculated Structure Factors of (II)

scale = 1 x $F_{absolute}$

$-F_{obs}$ indicates unobserved reflexion

K	L	OBS	CALC
**** H = 0 ****			
0	2	16	28
0	4	205	-230
0	6	669	715
0	8	295	293
0	10	207	-203
0	12	103	290
0	14	329	294
0	16	-21	-9
0	18	161	147
0	20	212	179
0	22	71	62
1	1	31	35
1	2	55	-58
1	3	188	207
1	4	110	126
1	5	180	195
1	6	-10	-14
1	7	-11	-9
1	8	58	-65
1	9	-14	6
1	10	193	183
1	11	171	166
1	12	92	79
1	13	44	27
1	14	206	-187
1	15	-17	13
1	16	76	63
1	17	117	102
1	18	177	159
1	19	121	99
1	20	162	-129
1	21	61	55
1	22	68	-60
1	23	52	38
2	0	-7	25
2	1	110	-130
2	2	24	22
2	3	47	-65
2	4	-10	-4
2	5	123	143
2	6	53	61
2	7	91	97
2	8	43	-32
2	9	235	-231
2	10	-12	12
2	11	41	-41
2	12	80	70
2	13	192	173
2	14	-16	-5
2	15	36	-24
2	16	-16	-16
2	17	133	-115
2	18	83	74
2	19	75	64
2	20	44	33
2	21	67	52
2	22	-16	-6
3	1	19	20
3	2	102	-121
3	3	46	-56
3	4	-11	22
3	5	130	-146
3	6	92	100
3	7	-11	13
3	8	170	-172
3	9	47	48
3	10	82	81
3	11	174	-161
3	12	96	96
3	13	85	-77
3	14	169	-151
3	15	111	100
3	16	13	20
3	17	77	-61
3	18	194	167
3	19	179	-151
3	20	156	-126
3	21	-17	9
4	0	586	-651
4	1	111	144
4	2	43	-52
4	3	31	42
4	4	155	174
4	5	151	-165
4	6	432	-482
4	7	23	26
4	8	233	-233
4	9	80	82
4	10	154	147
4	11	47	-37
4	12	263	-246
4	13	-14	8
4	14	304	-276
4	15	33	40
4	16	23	22
4	17	-17	-1
4	18	140	-121
4	19	-17	-9
4	20	192	-156
5	1	53	-66
5	2	-12	-25
5	3	133	-152
5	4	62	-66
5	5	89	-95
5	6	41	44
5	7	48	-59
5	8	48	49
5	9	89	-87
5	10	154	-149
5	11	134	-127
5	12	-15	-5
5	13	-15	-14
5	14	165	150
5	15	78	-64
5	16	52	-51
5	17	102	-93
5	18	119	-95
5	19	44	-34
6	0	90	-86
6	1	63	61
6	2	24	7
6	3	45	46
6	4	68	-76
6	5	114	-121
6	6	87	-92
6	7	63	-59
6	8	28	10
6	9	106	103
6	10	54	-50
6	11	-15	0
6	12	119	-120
6	13	107	-90
6	14	-15	2
6	15	61	61
6	16	-15	16
6	17	68	57
7	1	-15	13
7	2	88	109
7	3	-15	-4
7	4	91	-93
7	5	72	68
7	6	52	-55
7	7	-15	13
7	8	103	110
7	9	73	-87
7	10	45	-46
7	11	74	70
7	12	83	-73
7	13	79	67
7	14	56	85
8	0	296	292
8	1	93	-117
8	2	-15	21
8	3	42	-51
8	4	53	-53
8	5	151	168
8	6	213	231
8	7	46	-51
8	8	123	120
8	9	89	-89
**** H = 1 ****			
0	0	83	-74
0	2	174	158
0	4	128	125
0	6	24	-31
0	8	168	-167
0	10	273	294
0	12	31	36
0	14	128	-136
0	16	54	57
0	18	87	88
0	20	83	-78
0	22	-14	-14
1	0	188	-171
1	1	103	95
1	2	211	-165
1	3	103	100
1	4	-7	-3
1	5	114	-119
1	6	38	-35
1	7	141	139
1	8	120	-128
1	9	148	151
1	10	95	-106
1	11	177	-187
1	12	31	36
1	13	-11	9
1	14	74	-75
1	15	173	176
1	16	164	-166
1	17	92	-87
1	18	-14	0
1	19	86	-78
1	20	-17	18
1	21	202	180
1	22	104	-84
2	0	58	52
2	1	355	361
2	2	67	-59
2	3	524	-512
2	4	16	16
2	5	394	-393
2	6	87	89
2	7	182	194
2	8	23	-24
2	9	216	-225
2	10	55	-55
2	11	414	-450
2	12	68	73
2	13	34	27
2	14	38	-40
2	15	107	-100
2	16	-15	-30
2	17	271	-255
2	18	-15	19
2	19	61	-56
2	20	-15	-21
2	21	111	-102
2	22	-17	-6
3	0	205	-200
3	1	82	-81
3	2	-8	-10
3	3	-8	1
3	4	35	-31
3	5	50	54
3	6	81	-80
3	7	86	-88
3	8	136	-142
3	9	38	-40
3	10	54	-55
3	11	160	171
3	12	28	-2
3	13	-12	-24
3	14	151	-154
3	15	158	-162
3	16	95	-101
3	17	101	95
3	18	-15	-28
3	19	56	57
3	20	-20	-46
3	21	180	-166
4	0	37	34
4	1	89	-82
4	2	141	-147
4	3	88	-97
4	4	72	-64
4	5	-9	-9
4	6	135	142
4	7	21	-23
4	8	44	37
4	9	115	-112
4	10	124	-125
4	11	43	-46
4	12	19	15
4	13	-12	15
4	14	110	116
4	15	63	-62
4	16	69	-70
4	17	57	-50
4	18	64	-62
4	19	23	25
4	20	72	65
5	0	52	50
5	1	42	-38
5	2	104	101
5	3	109	-103
5	4	20	12
5	5	108	106
5	6	132	-131
5	7	59	-52
5	8	88	93
5	9	119	-117
5	10	80	91
5	11	96	97
5	12	99	-109
5	13	-13	-19
5	14	-13	20
5	15	140	-135
5	16	135	139
5	17	44	40
5	18	-14	-8
6	0	96	-86
6	1	184	-172
6	2	170	162
6	3	351	346
6	4	-12	-12
6	5	275	274
6	6	174	-169
6	7	132	-133
6	8	110	111
6	9	158	162
6	10	31	28
6	11	236	260
6	12	94	-95
6	13	20	-16
6	14	-13	16
6	15	55	54
6	16	42	37
7	0	129	129
7	1	-11	3
7	2	86	84
7	3	25	-25
7	4	29	23
7	5	-11	3
7	6	55	96
7	7	76	80
7	8	100	99
7	9	-13	-9
7	10	22	21
7	11	85	-88
7	12	48	46
7	13	54	57
8	0	23	-25
8	1	68	62
8	2	92	91
8	3	76	74
8	4	21	19
8	5	-12	5
8	6	96	-91
8	7	44	48
8	8	22	15
8	9	52	87
**** H = 2 ****			
0	0	468	-466
0	2	655	-666
0	4	157	193
0	6	251	-236
0	8	461	-567
0	10	-9	5
0	12	24	-26
0	14	353	-366
0	16	99	-68
0	18	34	-40
0	20	181	-183
1	0	110	-106
1	1	22	17
1	2	93	89
1	3	17	-14
1	4	31	-31
1	5	202	-196
1	6	90	-96
1	7	118	-118
1	8	142	141
1	9	42	44
1	10	-10	-10
1	11	115	-116
1	12	221	-226
1	13	126	-128
1	14	66	68
1	15	-12	8
1	16	51	59
1	17	27	-29
1	18	177	-189
1	19	76	-85
1	20	41	-41
1	21	66	-61
2	0	66	-60
2	1	80	-77
2	2	32	-33
2	3	69	69
2	4	27	-27
2	5	29	28
2	6	17	-17
2	7	158	-157
2	8	-9	5
2	9	-9	-19
2	10	-10	6
2	11	139	141
2	12	20	-16
2	13	52	-97
2	14	24	-18
2	15	84	-98
2	16	21	15
2	17	55	60
2	18	-12	4
2	19	-12	19
2	20	54	-59
3	0	100	-93
3	1	16	-15
3	2	22	25
3	3	36	-33
3	4	19	-25
3	5	56	54
3	6	141	-136
3	7	53	90
3	8	127	127
3	9	48	-46
3	10	-10	-1
3	11	31	33
3	12	186	-187
3	13	173	177
3	14	41	46
3	15	-12	-6
3	16	87	97
3	17	56	-67
3	18	165	-175
3	19	52	98
3	20	47	-50
4	0	345	339
4	1	-9	1
4	2	427	414
4	3	154	-148
4	4	180	-176
4	5	80	73
4	6	128	123
4	7	56	55
4	8	418	416
4	9	84	-81
4	10	-11	0
4	11	-11	15
4	12	-11	10
4	13	25	26
4	14	265	279
4	15	42	-47
4	16	74	83
4	17	22	-19
4	18	33	28
5	0	26	-23
5	1	19	-20
5	2	-10	-12
5	3	87	87
5	4	86	80
5	5	161	155
5	6	32	33
5	7	82	75
5	8	102	-100
5	9	20	18
5	10	34	34
5	11	130	133
5	12	131	133
5	13	87	91
5	14	47	-40
5	15	30	30
5	16	65	-71
5	17	96	67
6	0	67	63
6	1	-11	21
6	2	46	41
6	3	84	-86
6	4	20	20
6	5	-11	3
6	6	102	98
6	7	113	115
6	8	34	27
6	9	21	22
6	10	-12	-17
6	11	67	-67
6	12	81	82
6	13	60	61
6	14	79	85
6	15	67	72
7	0	90	85
7	1	-11	-3
7	2	58	-54
7	3	40	44
7	4	19	15
7	5	-11	-19
7	6	126	126
7	7	55	-91
7	8	35	-38
7	9	59	61
7	10	26	-21
7	11	33	34
8	0	168	-165
8	1	-12	-8
8	2	226	-220
8	3	185	178
8	4	100	95
8	5	50	-45
8	6	64	-61
**** H = 3 ****			
0	0	204	195
0	2	100	-91
0	4	106	-105
0	6	63	-69
0	8	92	89
0	10	70	-70
0	12	189	-184
0	14	55	59
0	16	20	19
0	18	117	-125
0	20	24	-22
1	0	33	33
1	1	50	-48
1	2	128	130
1	3	125	-127
1	4	104	101
1	5	76	72
1	6	-9	-20
1	7	-9	6
1	8	91	92
1	9	238	-237
1	10	158	160
1	11	26	-23
1	12	-11	15
1	13	59	101
1	14	46	-44
1	15	151	-142
1	16	160	109
1	17	96	-94
1	18	86	96
1	19	128	138
2	0	98	-92
2	1	220	-209
2	2	32	31
2	3	60	55
2	4	35	32
2	5	602	582
2	6	78	-75
2	7	-9	11
2	8	50	-51
2	9	102	-104
2	10	37	41
2	11	384	374
2	12	17	-12
2	13	157	154
2	14	29	-35
2	15	46	-44
2	16	-12	17
2	17	168	183
2	18	-12	8
2	19	86	95
3	0	92	87
3	1	39	40
3	2	151	148
3	3	81	79
3	4	30	30
3	5	81	-75
3	6	56	51
3	7	30	32
3	8	62	59
3	9	186	181
3	10	135	135
3	11	40	-40
3	12	-11	9
3	13	54	-93
3	14	25	28
3	15	157	160
3	16	81	87
3	17	56	59
3	18	58	64
4	0	55	-47
4	1	-9	10
4	2	35	30
4	3	51	51
4	4	160	159
4	5	62	58
4	6	47	31
4	7	38	-36
4	8	80	-81
4	9	54	52
4	10	76	74
4	11	101	103
4	12	120	118
4	13	25	-27
4	14	45	-45
4	15	23	20
4	16	22	-15
4	17	91	100
5	0	25	23
5	1	-10	10
5	2	60	-55
5	3	145	144
5	4	119	-114
5	5	33	-31
5	6	23	28
5	7	73	-72
5	8	44	42
5	9	179	177
5	10	145	-143
5	11	29	25
5	12	-11	3
5	13	84	-82
5	14	114	115
5	15	102	106
6	0	158	154
6	1	86	76
6	2	-11	2
6	3	-12	-10
6	4	129	-130
6	5	301	-347
6	6	132	126
6	7	52	-54
6	8	60	54
6	9	41	39
6	10	94	-91
6	11	229	-223
6	12	47	43
6	13	103	-102
7	0	60	-52
7	1	24	-22
7	2	103	-100
7	3	-11	-1
7	4	64	-60
7	5	61	60
7	6	45	-37
7	7	-12	-18
7	8	81	-75
7	9	107	-107
8	0	58	53
8	1	23	-17
8	2	35	-28
**** H = 4 ****			
0	0	145	-143
0	2	586	575
0	4	162	157
0	6	148	-143
0	8	307	302
0	10	278	277
0	12	94	-76
0	14	143	152
0	16	166	174
0	18	-12	7
1	0	99	99
1	1	98	86
1	2	16	-10
1	3	26	19
1	4	15	-16
1	5	56	66
1	6	181	183
1	7	120	120
1	8	25	21
1	9	40	40
1	10	137	-139
1	11	-11	-14
1	12	136	142
1	13	78	79
1	14	116	121
1	15	65	72
1	16	130	-138
1	17	23	1
2	0	48	49
2	1	203	197
2	2	24	24
2	3	53	51
2	4	-10	2
2	5	56	-56
2	6	48	50
2	7	76	75
2	8	42	44
2	9	159	193
2	10	-11	-24
2	11	33	-36
2	12	-11	6
2	13	52	-54
2	14	32	27
2	15	123	125
2	16	-11	15
2	17	60	63
3	0	189	183
3	1	80	-75
3	2	64	62
3	3	20	20
3	4	66	-64
3	5	-10	5
3	6	188	189
3	7	112	-110
3	8	74	70
3	9	21	-12
3	10	117	-111
3	11	100	101
3	12	128	132
3	13	64	-73
3	14	108	111
3	15	110	-117
3	16	85	-87
4	0	80	77
4	1	117	-111
4	2	458	-446
4	3	73	67
4	4	112	-102
4	5	81	77
4	6	146	144
4	7	-11	-78
4	8	268	-266
4	9	-11	2
4	10	188	-186
4	11	52	51
4	12	73	71
4	13	34	-35
4	14	111	-115
4	15	-12	11
5	0	31	-31
5	1	42	-37
5	2	67	62
5	3	40	-36
5	4	35	-35
5	5	81	-78
5	6	136	-136
5	7	69	-66
5	8	-10	19
5	9	31	-30
5	10	63	61
5	11	56	-57
5	12	-13	-102
5	13	81	-81
6	0	50	-47
6	1	120	-114
6	2	49	-47
6	3	-11	-6
6	4	-11	11
6	5	51	47
6	6	59	-56
6	7	61	-61
6	8	78	-74
6	9	99	-92
6	10	-12	2
7	0	127	-118
7	1	45	49
7	2	19	-27
7	3	23	-15
7	4	54	53
7	5	62	-58
**** H = 5 ****			
0	0	82	76
0	2	56	-60
0	4	44	46
0	6	162	160
0	8	17	35
0	10	88	-87
0	12	119	123
0	14	78	82
1	0	-10	6
1	1	30	-33
1	2	-10	-4
1	3	154	153
1	4	92	-84
1	5	67	72
1	6	-11	-19
1	7	100	-101
1	8	59	53
1	9	100	106
1	10	75	-76
1	11	145	150
1	12	100	-102
1	13	68	-69
1	14	24	23
1	15	25	20
2	0	28	28
2	1	251	-232
2	2	54	53
2	3	219	217
2	4	58	-59
2	5	238	-235
2	6	21	21
2	7	277	-284
2	8	43	48
2	9	109	106
2	10	-11	0
2	11	76	-75
2	12	-11	16
2	13	221	-224
2	14	28	27
3	0	-10	6
3	1	-10	-3
3	2	117	-121
3	3	138	-138
3	4	69	-64
3	5	28	-33
3	6	-10	-7
3	7	91	96
3	8	-11	-14
3	9	103	-102
3	10	58	-95
3	11	113	-113
3	12	54	-53
3	13	97	99
4	0	43	-40
4	1	-10	0
4	2	22	19
4	3	-10	-1
4	4	64	-69
4	5	64	-63
4	6	146	-146
4	7	-11	-13
4	8	-11	0
4	9	23	28
4	10	43	41
4	11	60	-59
5	0	40	-30
5	1	30	31
5	2	-11	-23
5	3	93	-94
5	4	57	61
5	5	90	-96
5	6	48	46
5	7	67	65
5	8	72	-75
5	9	67	-64
6	0	73	-69
6	1	133	126
6	2	111	-106
6	3	131	-126
6	4	94	82
6	5	144	148
**** H = 6 ****			
0	0	221	225
0	2	143	-142
0	4	302	-295
0	6	85	83
0	8	33	-26
0	10	269	-269
1	0	98	-99
1	1	84	-88
1	2	70	-71
1	3	-11	4
1	4	74	74
1	5	18	-18
1	6	75	-78
1	7	68	-70
1	8	128	-131
1	9	69	-71
1	10	65	65
1	11	-11	-5
2	0	-10	-4
2	1	107	-103
2	2	24	-22
2	3	112	-118
2	4	27	-21
2	5	22	-25
2	6	-10	1
2	7	22	24
2	8	40	-42
2	9	91	-97
2	10	23	-23
3	0	87	-84
3	1	56	60
3	2	103	-107
3	3	32	35
3	4	50	52
3	5	38	-43
3	6	46	-62
3	7	37	39
3	8	168	-172
3	9	99	99
4	0	164	-164
4	1	32	27
4	2	115	116
4	3	-12	18
4	4	275	280
4	5	88	-85
4	6	76	-77
4	7	-11	-7
5	0	69	71
5	1	72	73
5	2	-11	4
5	3	-11	-12
**** H = 7 ****			
0	0	127	-132
0	2	20	-18
0	4	17	9
0	6	89	-88
1	0	-11	-1
1	1	48	50
1	2	-11	-7
1	3	26	-29
1	4	39	38
1	5	162	-161
2	0	34	35
2	1	327	329
2	2	82	-60
2	3	59	-62
2	4	-11	1
3	0	-11	3
3	1	49	-41
**** H = -1 ****			
0	2	125	-112
0	4	142	129
0	6	114	113
0	8	230	-225
0	10	87	-89
0	12	217	229
0	14	-12	-7
0	16	77	-76
0	18	84	84
0	20	124	113
0	22	70	-63
1	1	116	-103
1	2	38	37
1	3	80	78
1	4	-7	11
1	5	69	63
1	6	159	159
1	7	208	-208
1	8	142	146
1	9	114	119
1	10	-10	-20
1	11	142	152
1	12	-10	-3
1	13	179	-189
1	14	172	188
1	15	-17	-14
1	16	-12	9
1	17	185	184
1	18	76	-65
1	19	81	-78
1	20	71	75
1	21	124	-109
1	22	118	103
1	23	172	146
2	1	244	231
2	2	19	18
2	3	765	772
2	4	76	-76
2	5	49	-50
2	6	-5	14
2	7	15	-16
2	8	110	114
2	9	588	604
2	10	34	-37
2	11	169	173
2	12	25	-17
2	13	125	-140
2	14	68	72
2	15	241	304
2	16	-13	-1
2	17	212	207
2	18	-14	-7
2	19	-13	4
2	20	-14	-4
2	21	147	138
2	22	-16	-6
3	1	15	-15
3	2	50	47
3	3	43	-40
3	4	-7	24
3	5	49	-42
3	6	159	158
3	7	44	41
3	8	169	176
3	9	78	-75
3	10	-10	-13
3	11	76	-68
3	12	127	135
3	13	109	181
3	14	127	139
3	15	-13	6
3	16	30	35
3	17	155	-158
3	18	41	37
3	19	111	101
3	20	87	78
3	21	108	99
4	1	40	40
4	2	33	29
4	3	-8	4
4	4	148	-142
4	5	17	22
4	6	99	-91
4	7	87	84
4	8	102	100
4	9	55	59
4	10	48	47
4	11	-12	-1
4	12	144	-155
4	13	-13	21
4	14	-13	1
4	15	87	90
4	16	57	94
4	17	-13	-4
4	18	83	-80
4	19	23	-26
4	20	71	-63
5	1	110	107
5	2	12	-24
5	3	62	-59
5	4	18	17
5	5	104	-104
5	6	20	-18
5	7	167	167
5	8	142	-140
5	9	31	-29
5	10	40	43
5	11	114	-125
5	12	52	61
5	13	103	111
5	14	107	-116
5	15	57	61
5	16	53	-59
5	17	137	-140
5	18	111	101
5	19	41	36
6	1	142	-130
6	2	100	-96
6	3	456	-454
6	4	158	153
6	5	43	36
6	6	-12	-10
6	7	21	22
6	8	143	-145
6	9	302	-311
6	10	63	61
6	11	75	-80
6	12	40	46
6	13	46	47
6	14	70	-68
6	15	163	-171
6	16	-14	-11
6	17	130	-123
7	1	88	29
7	2	53	-46
7	3	-11	8
7	4	51	-45
7	5	51	-58
7	6	100	-96
7	7	20	-25
7	8	71	-73
7	9	48	54
7	10	29	-29
7	11	-13	-1
7	12	79	-75
7	13	84	-96
7	14	78	-81
8	1	65	-63
8	2	38	-39
8	3	21	-25
8	4	85	81
8	5	-12	-2
8	6	47	51
8	7	86	-82
8	8	77	-75
8	9	65	-67
**** H = -2 ****			
0	2	436	412
0	4	392	-371
0	6	550	-530
0	8	93	93
0	10	60	-64
0	12	473	-469
0	14	45	-42
0	16	-11	-13
0	18	234	-250
0	20	113	-118
0	22	36	-34
1	1	181	-173
1	2	13	12
1	3	170	-165
1	4	38	-38
1	5	31	-32
1	6	60	61
1	7	46	39
1	8	35	32
1	9	119	-142
1	10	111	-109
1	11	158	-156
1	12	117	111
1	13	33	31
1	14	84	93
1	15	87	-90
1	16	161	-170
1	17	132	-142
1	18	29	30
1	19	39	-35
1	20	156	177
1	21	24	-14
1	22	174	-120
1	23	74	-71
2	1	104	105
2	2	-8	-1
2	3	45	39
2	4	76	-27
2	5	57	40
2	6	56	-50
2	7	115	113
2	8	-9	26
2	9	164	167
2	10	61	-60
2	11	119	-124
2	12	-12	-7
2	13	-11	-14
2	14	-11	-1
2	15	149	158
2	16	52	-60
2	17	-12	-14
2	18	42	-44
2	19	57	-63
2	20	-13	10
2	21	71	85
2	22	-13	-18
3	1	29	28
3	2	147	135
3	3	110	122
3	4	99	-93
3	5	18	42
3	6	131	128
3	7	22	-17
3	8	-9	82
3	9	114	118
3	10	144	-141
3	11	132	132
3	12	107	106
3	13	36	-38
3	14	52	99
3	15	-12	13
3	16	157	-167
3	17	129	142
3	18	-12	11
3	19	29	25
3	20	150	172
3	21	71	-71
4	1	157	-147
4	2	283	-271
4	3	125	117
4	4	250	236
4	5	72	76
4	6	498	495
4	7	150	-152
4	8	87	-83
4	9	25	25
4	10	80	80
4	11	84	84
4	12	362	387
4	13	42	-60
4	14	57	62
4	15	-12	5
4	16	-12	-6
4	17	54	54
4	18	185	200
4	19	-17	-10
4	20	85	93
5	1	150	141
5	2	-11	-21
5	3	146	142
5	4	-10	-5
5	5	38	32
5	6	74	-75
5	7	-11	15
5	8	48	46
5	9	143	148
5	10	60	59
5	11	89	88
5	12	134	-129
5	13	-12	-17
5	14	31	-29
5	15	94	104
5	16	120	129
5	17	-13	80
5	18	31	-31
5	19	21	22
6	1	116	-117
6	2	39	44
6	3	45	47
6	4	58	97
6	5	84	86
6	6	-11	8
6	7	137	-133
6	8	-11	20
6	9	82	-82
6	10	80	82
6	11	80	84
6	12	46	45
6	13	-12	-19
6	14	28	-33
6	15	104	-109
6	16	66	74
7	1	-11	-3
7	2	34	-26
7	3	20	-18
7	4	70	67
7	5	32	-32
7	6	71	-71
7	7	69	67
7	8	69	-61
7	9	-12	-8
7	10	87	85
7	11	94	-95
7	12	50	-52
7	13	54	56
8	1	164	138
8	2	124	119
8	3	127	-119
8	4	132	-123
8	5	92	-86
8	6	242	-238
8	7	156	155
8	8	28	28
**** H = -3 ****			
0	2	-8	-16
0	4	189	-184
0	6	-11	4
0	8	93	95
0	10	221	-223
0	12	172	-170
0	14	34	37
0	16	22	-20
0	18	121	-124
0	20	33	-27
0	22	30	40
1	1	84	80
1	2	48	41
1	3	88	-89
1	4	45	-43
1	5	36	-31
1	6	136	-137
1	7	51	49
1	8	-9	-5
1	9	190	-190
1	10	49	44
1	11	-10	-9
1	12	129	-131
1	13	104	108
1	14	76	-79
1	15	164	-156
1	16	40	42
1	17	74	-77
1	18	51	-59
1	19	146	154
1	20	101	-103
1	21	55	-56
1	22	39	-41
2	1	600	-622
2	2	22	19
2	3	281	-269
2	4	20	20
2	5	244	239
2	6	-7	-52
2	7	332	-321
2	8	20	-16
2	9	407	-399
2	10	46	42
2	11	104	105
2	12	35	-33
2	13	124	-125
2	14	25	-17
2	15	337	-338
2	16	-12	12
2	17	25	-35
2	18	-12	16
2	19	41	-45
2	20	-12	-16
2	21	156	-165
3	1	-9	-1
3	2	32	24
3	3	82	84
3	4	172	-167
3	5	-9	0
3	6	167	-155
3	7	-9	-3
3	8	-10	10
3	9	115	116
3	10	72	-71
3	11	53	-50
3	12	184	-184
3	13	85	-89
3	14	-11	-13
3	15	144	144
3	16	-11	-18
3	17	33	32
3	18	79	-86
3	19	132	-142
3	20	78	-84
3	21	60	63
4	1	33	-31
4	2	51	56
4	3	-10	-6
4	4	155	146
4	5	62	-58
4	6	-10	-5
4	7	94	-90
4	8	71	-62
4	9	15	-1
4	10	149	151
4	11	16	10
4	12	120	122
4	13	61	-57
4	14	94	-99
4	15	38	-38
4	16	36	40
4	17	39	38
4	18	106	111
4	19	32	-40
5	1	70	-68
5	2	-10	-11
5	3	114	116
5	4	-10	-6
5	5	40	45
5	6	70	72
5	7	78	-76
5	8	34	35
5	9	111	129
5	10	-12	-91
5	11	33	33
5	12	57	54
5	13	80	-81
5	14	124	127
5	15	104	105
5	16	53	-56
5	17	88	85
5	18	27	-29
6	1	362	355
6	2	39	-31
6	3	158	150
6	4	85	-85
6	5	185	-180
6	6	141	138
6	7	186	184
6	8	30	27
6	9	250	245
6	10	103	-101
6	11	70	-69
6	12	45	43
6	13	58	62
6	14	65	76
6	15	227	231
7	1	-11	1
7	2	28	26
7	3	-11	15
7	4	90	87
7	5	-11	13
7	6	91	86
7	7	33	-38
7	8	-11	14
7	9	11	-34
7	10	47	44
7	11	49	49
7	12	119	119
8	1	42	40
8	2	55	-52
8	3	25	28
8	4	89	-85
8	5	71	70
**** H = -4 ****			
0	2	111	-111
0	4	399	381
0	6	180	171
0	8	263	-263
0	10	301	302
0	12	328	315
0	14	119	-118
0	16	151	156
0	18	232	240
0	20	39	44
1	1	161	161
1	2	-9	4
1	3	38	36
1	4	-9	-4
1	5	39	-36
1	6	93	-89
1	7	75	67
1	8	25	24
1	9	157	157
1	10	-10	-5
1	11	-10	-3
1	12	179	-181
1	13	-11	5
1	14	64	61
1	15	139	142
1	16	58	62
1	17	50	52
1	18	176	-186
1	19	-11	1
1	20	40	-26
1	21	54	41
2	1	74	-67
2	2	-9	-2
2	3	53	48
2	4	40	36
2	5	64	-61
2	6	-9	-1
2	7	176	-171
2	8	25	28
2	9	15	31
2	10	41	43
2	11	92	88
2	12	-10	5
2	13	153	-158
2	14	-11	17
2	15	100	-105
2	16	42	44
2	17	65	66
2	18	19	10
2	19	50	-55
2	20	-12	-22
3	1	114	-113
3	2	54	50
3	3	50	-47
3	4	29	23
3	5	31	27
3	6	191	-189
3	7	49	-45
3	8	41	61
3	9	116	-114
3	10	25	22
3	11	-11	3
3	12	131	-134
3	13	55	59
3	14	-11	12
3	15	84	-89
3	16	72	73
3	17	75	-75
3	18	138	-147
3	19	59	59
4	1	29	-24
4	2	80	60
4	3	156	-149
4	4	506	-489
4	5	61	56
4	6	109	-104
4	7	67	64
4	8	146	141
4	9	132	-127
4	10	249	-266
4	11	-11	-8
4	12	219	-212
4	13	50	48
4	14	90	86
4	15	46	-45
4	16	97	-101
4	17	25	-21
4	18	153	-199
5	1	114	-111
5	2	34	34
5	3	49	-44
5	4	-10	-2
5	5	18	-16
5	6	20	18
5	7	76	-77
5	8	41	-41
5	9	109	-103
5	10	53	55
5	11	19	15
5	12	53	91
5	13	-10	-67
5	14	67	-65
5	15	104	-102
5	16	48	-46
6	1	-12	12
6	2	39	-36
6	3	73	-72
6	4	26	-26
6	5	86	81
6	6	25	-19
6	7	131	126
6	8	48	-46
6	9	33	-29
6	10	65	-70
6	11	19	-7
6	12	-12	-9
6	13	136	138
7	1	-11	-5
7	2	31	-24
7	3	-11	10
7	4	22	-22
7	5	-11	-14
7	6	143	138
7	7	35	-37
7	8	-11	5
**** H = -5 ****			
0	2	194	193
0	4	42	43
0	6	-10	-15
0	8	127	122
0	10	213	210
0	12	38	-42
0	14	23	-17
0	16	155	154
0	18	78	84
1	1	16	19
1	2	30	27
1	3	149	145
1	4	124	125
1	5	36	-41
1	6	41	40
1	7	48	47
1	8	42	-45
1	9	140	140
1	10	76	74
1	11	91	-91
1	12	113	111
1	13	40	38
1	14	15	-17
1	15	171	177
1	16	17	8
1	17	79	-80
1	18	53	97
1	19	31	-56
2	1	425	427
2	2	69	-65
2	3	187	-179
2	4	34	33
2	5	67	58
2	6	47	43
2	7	456	446
2	8	35	-35
2	9	32	31
2	10	-11	-1
2	11	59	-100
2	12	58	55
2	13	291	286
2	14	18	-4
2	15	147	144
2	16	28	-28
2	17	83	-78
2	18	-12	13
3	1	28	-28
3	2	57	57
3	3	65	-63
3	4	134	132
3	5	-11	9
3	6	70	68
3	7	37	-30
3	8	-11	-11
3	9	25	-24
3	10	90	94
3	11	70	71
3	12	79	82
3	13	59	-59
3	14	21	-25
3	15	99	-101
3	16	44	48
3	17	84	84
4	1	30	33
4	2	153	-147
4	3	31	28
4	4	56	-57
4	5	55	55
4	6	54	59
4	7	-10	2
4	8	45	-88
4	9	18	-14
4	10	143	-141
4	11	52	55
4	12	50	53
4	13	41	46
4	14	-11	10
4	15	20	-15
4	16	142	-142
5	1	56	-55
5	2	39	-39
5	3	144	-138
5	4	45	-45
5	5	51	57
5	6	38	-32
5	7	65	-65
5	8	41	43
5	9	158	-156
5	10	-12	9
5	11	65	61
5	12	57	-98
5	13	18	-7
6	1	265	-265
6	2	106	105
6	3	114	108
6	4	43	-38
6	5	29	11
6	6	129	-127
6	7	103	-235
6	8	78	79
6	9	34	-35
**** H = -6 ****			
0	2	261	-256
0	4	258	-301
0	6	183	183
0	8	65	-61
0	10	389	-388
0	12	-14	22
0	14	-11	17
0	16	258	-256
1	1	58	-57
1	2	-11	-13
1	3	64	66
1	4	80	78
1	5	35	-38
1	6	97	93
1	7	132	-134
1	8	34	-30
1	9	28	-22
1	10	57	98
1	11	35	37
1	12	63	60
1	13	58	-93
1	14	76	-79
1	15	70	-63
1	16	89	87
2	1	-11	-17
2	2	-11	-13
2	3	43	47
2	4	-11	-15
2	5	142	142
2	6	-11	2
2	7	57	55
2	8	-11	-19
2	9	35	-32
2	10	-11	-7
2	11	118	118
2	12	-11	-7
2	13	130	132
2	14	-11	-7
2	15	28	-28
3	1	-11	12
3	2	35	-38
3	3	-11	-11
3	4	56	97
3	5	-11	15
3	6	78	79
3	7	69	71
3	8	50	-52
3	9	29	16
3	10	50	90
3	11	52	-48
3	12	81	82
3	13	30	32
3	14	57	-57
4	1	55	95
4	2	224	226
4	3	36	33
4	4	245	253
4	5	71	-73
4	6	146	-142
4	7	46	51
4	8	55	41
4	9	77	79
4	10	276	277
4	11	-11	-53
4	12	-11	-3
5	1	75	78
5	2	-11	-6
5	3	32	-30
5	4	21	-17
5	5	33	35
5	6	20	-22
5	7	122	119
5	8	22	-16
**** H = -7 ****			
0	2	58	-93
0	4	25	-18
0	6	30	-33
0	8	160	-170
0	10	81	-79
0	12	54	54
1	1	103	-103
1	2	62	-65
1	3	62	-65
1	4	44	-47
1	5	19	23
1	6	49	46
1	7	112	-112
1	8	-12	-15
1	9	42	-42
1	10	87	-90
1	11	24	29
2	1	55	-52
2	2	-11	15
2	3	156	163
2	4	49	-46
2	5	238	-241
2	6	-11	-7
2	7	150	-190
2	8	23	25
2	9	137	146
2	10	33	-34
3	1	44	39
3	2	75	-79
3	3	31	35
3	4	46	-46
3	5	-11	-4
3	6	25	26
3	7	53	55

3.6.3 Structural Analysis of α-$(CH_3)_2TeI_2$

Of the 3157 intensities measured for α-$Te(CH_3)_2I_2$, 2191 were above 2.5σ and were considered as observed. The Tangent Refinement Programs were applied to reflexions with E values above 1.80 (E_{max}=3.65). The origin-determining reflexions were 5 5 -11 (E=3.65) 7 0 -4 (E=3.42) and 7 12 -1 (E=2.90). Two additional reflexions 5 11 7 (E=3.57) and 3 11 -1 (E=3.14) were used to help initiate phase assignments. Of the four combinations of signs, (+) 5 11 -7 and (-) 3 11 -1 had the lowest R_{karle} (Section 3.2.2) values of 0.12 after 10 cycles of phase refinement (others being 0.20, 0.24 and 0.39).

A Fourier map using the 238 signed E's as coefficients revealed clearly all the nine heavy atoms in the asymmetric unit . From the geometry of the atomic arrangement six iodine and three tellurium atoms were assigned. Initial refinement commenced at a conventional R value of 0.223 and dropped to 0.119 after four cycles of full matrix least-squares refinement. An electron density difference map revealed the six carbon atomic positions. Two further cycles of refinement brought the R down to 0.105 with isotropic thermal parameters for all the atoms. Another electron density difference map showed anisotropic thermal motion about the six iodine atoms to be substantial and

introduction of the appropriate variables led R to 0.072. Secondary extinction effects were observed and the parameter E_c was introduced (section 3.4.4, final E_c value being $2.2(2) \times 10^{-6}$) with R subsequently dropping to 0.068. Another electron density difference map suggested inclusion of anisotropic thermal parameters of the three tellurium atoms, leading to an R= 0.063. Unit weight had been used up to this point. Analysis showed that the lower and higher F's were overweighted. A weighting scheme such as described in (20) was constructed. The final numerical values were $\sigma = 440/F_{obs}$ for $F_{obs} \leq 80$, $\sigma = 0.502 \sqrt{F_{obs}}$ for $F_{obs} > 150$ and $\sigma = 5.5$ for $80 < F_{obs} \leq 150$. Refinement of the model by two more cycles using this weighting scheme was considered complete at R=0.054 and R_w=0.059. An electron density map computed at this point showed peaks and troughs no larger than ± 0.70 e/Å^3, the largest peak and trough occurring at 1.5 Å from Te(1) and 1.8 Å from I(2) respectively.

A calculation of the lower and upper bound limits (see section 3.5) of the Te-I distances showed that while the uncorrected values were not significantly different from the lower bound limits the upper limits were some 24σ above the uncorrected values. Though the anisotropic thermal parameters might contain errors

due to the approximate absorption correction, the values obtained are physically reasonable indicating that the motion of the iodine and tellurium atoms is mainly perpendicular to the Te-I bonds. Two types of correction for thermal motion, the riding and the independent model (section 3.5), were considered. Results of computation are summarized in Table (XI). The correction obtained by regarding the motion as the iodine atoms riding on the tellurium atoms is small, about 3σ different from the uncorrected value. This model is also physically close to the lower bound limit situation[34] where the tellurium and iodine atoms possess highly correlated parallel displacements, which, in view of the linearity of the I-Te-I fragments, merely corresponds to rigid body motion (and exclude probable bending modes). Because of this the riding model probably underestimates the correction. One might expect that for linear I-Te-I groups the true bond lengths are intermediate between the upper and lower bound limit — a value similar to that obtained from the independent model. This model has been rejected, however, because it assumes the two bonded atoms to be completely uncorrelated. Hence values from the riding model are used throughout the discussion.

The packing of molecules in the unit cell is shown

TABLE XI. Corrections for Thermal Motion Effects for Te-I Bond Lengths

	lower bound limit	upper bound limit	uncorrected value	Riding model (I on Te)	Independent model
Te(1)-I(1)	2.957	3.026	2.956	2.965	2.991
Te(1)-I(2)	2.875	2.949	2.874	2.885	2.912
Te(2)-I(3)	2.902	2.981	2.899	2.914	2.941
Te(3)-I(4)	2.923	2.998	2.920	2.934	2.961
Te(3)-I(5)	2.846	2.917	2.845	2.854	2.882
Te(3)-I(6)	2.983	3.057	2.982	2.994	3.020

*Calculations based on expressions given in section 3.5

in Figure 4. Table (XII) lists the final atomic parameters, Table (XIII) the interatomic distances and angles and Table(XIV) the observed and calculated structure factors.

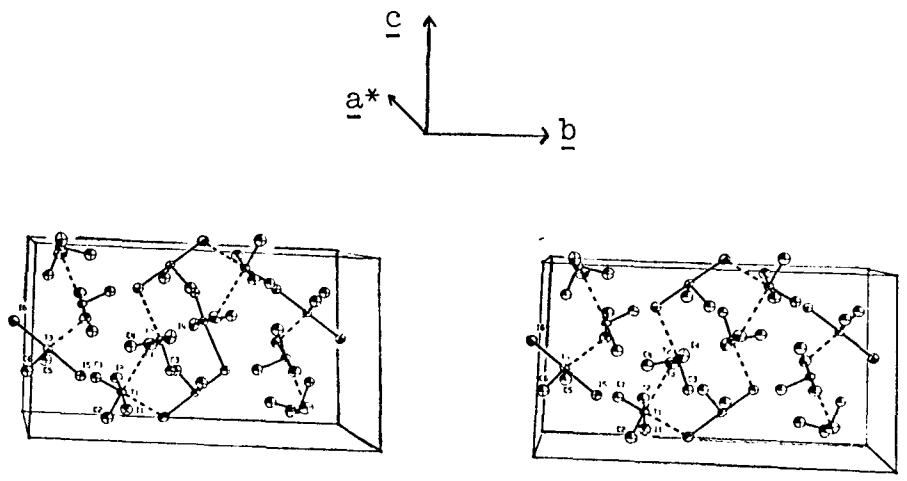

Figure 4. Stereomolecular packing diagrams viewed down an axis rotated by 8° from a* towards a. Short intermolecular Te...I contacts within the unit cell cell are shown as dotted lines. Thermal ellipsoids contain 50% electron density of the atoms.

TABLE XII. Final Positional and Thermal Parameters for α-$(CH_3)_2TeI_2$

Atom	x	y	z	B(Å^2)
I(1)	0.1333(3)	0.1838(1)	0.5544(1)	*
I(2)	-0.4247(2)	0.1876(1)	0.6661(2)	*
I(3)	0.0099(2)	0.1044(1)	0.9152(2)	*
I(4)	0.6512(2)	0.0850(1)	1.0143(2)	*
I(5)	0.3404(2)	0.1644(1)	0.2534(1)	*
I(6)	0.2605(2)	-0.0402(1)	0.5318(2)	*
Te(1)	-0.1459(2)	0.1848(1)	0.6165(1)	*
Te(2)	0.3292(2)	0.0925(1)	0.9657(1)	*
Te(3)	0.2967(2)	0.0647(1)	0.3880(1)	*
C(1)	-0.0868(31)	0.2699(13)	0.7004(23)	5.0(6)
C(2)	-0.2511(30)	0.2225(13)	0.4513(23)	4.9(6)
C(3)	0.3029(28)	0.0600(12)	0.7978(22)	4.3(6)
C(4)	0.3406(31)	0.1853(14)	0.9288(24)	5.2(6)
C(5)	0.0634(33)	0.0645(14)	0.3016(26)	5.8(7)
C(6)	0.3353(29)	0.0008(13)	0.2663(23)	4.7(6)

	U_{11} (Å^{2}x10^2)	U_{22}	U_{33}	U_{12}	U_{13}	U_{23}
I(1)	4.27(10)	7.00(12)	6.17(11)	-0.04(9)	2.25(9)	-0.43(10)
I(2)	4.77(10)	7.72(13)	6.17(12)	-0.12(10)	2.77(9)	0.15(10)
I(3)	4.50(10)	9.80(16)	7.07(13)	-0.71(11)	1.64(9)	-0.76(12)
I(4)	4.74(11)	6.38(13)	9.13(15)	0.16(10)	2.12(10)	0.37(11)
I(5)	7.68(13)	5.15(11)	4.81(11)	-0.49(10)	1.62(9)	-0.12(9)
I(6)	9.76(16)	5.73(12)	5.80(12)	-0.17(11)	3.47(11)	-0.76(10)
Te(1)	3.51(8)	4.61(10)	3.29(9)	-0.16(8)	0.82(7)	-0.19(8)
Te(2)	4.22(9)	4.37(10)	3.59(9)	-0.08(8)	1.37(7)	-0.12(8)
Te(3)	4.66(10)	4.43(10)	3.78(9)	-0.15(8)	1.29(8)	-0.73(8)

* Anisotropic thermal parameters used for iodine and tellurium atoms.

Table XIII. Interatomic distances (Å) and angles (°) for (III)

Te(1)		Te(2)		Te(3)		corresponding values for $(CH_3)TeCl_2$
Te - I(1)	2.965(3)‡	Te - I(3)	2.914(3)	Te - I(5)	2.854(3)	Te-Cl 2.42(1)
- I(2)	2.885(3)	- I(4)	2.934(3)	- I(6)	2.994(3)	2.54(1)
- C(1)	2.12(3)	- C(3)	2.12(3)	- C(5)	2.13(3)	2.08(3)
- C(2)	2.13(3)	- C(4)	2.10(3)	- C(6)	2.16(3)	2.10(3)
...I(3)*[1]	3.919(3)†	...I(4)[3]	3.912(3)	...I(1)[1]	3.907(3)	
...I(6)[2]	3.659(3)	...I(5)[4]	3.826(3)	...I(6)[2]	4.030(3)	
I(1)- Te - I(2)	177.3(2)	I(3)- Te - I(4)	178.0(2)	I(5) - Te - I(6)	178.3(6)	172.3(3)
C(1)- - C(2)	95(2)	C(3)- - C(4)	97(2)	C(5) - - C(6)	91(2)	98(1)
C(1)- ...I(3)	89(1)	C(3)- ...I(4)	73(1)	C(5) - ...I(1)	75(1)	
C(1)- ...I(6)	178(1)	C(3)- ...I(5)	173(1)	C(5) - ...I(6)	163(1)	
C(2)- ...I(6)	83(1)	C(4)- ...I(5)	79(1)	C(4) - ...I(6)	73(1)	
I(2)... ...I(3)	174(1)	C(4)- ...I(4)	168(1)	C(4) - ...I(1)	166(1)	
I(3)... ...I(6)	92(1)	I(4)... ...I(5)	112(1)	I(1)... ...I(6)	120(1)	
I(1)- - C(1)	90(1)	I(3)- - C(3)	91(1)	I(5) - - C(5)	91(1)	86(1)
I(1)- - C(2)	87(1)	I(3)- - C(4)	90(1)	I(5) - - C(6)	90(1)	88(1)
I(1)- ...I(3)	97(1)	I(3)- ...I(4)	97(1)	I(5) - ...I(1)	86(1)	
I(1)- ...I(6)	92(1)	I(3)- ...I(5)	84(1)	I(5) - ...I(6)	86(1)	
I(2)- - C(1)	90(1)	I(4)- - C(3)	89(1)	I(6) - - C(5)	90(1)	87(1)
I(2)- - C(2)	90(1)	I(4)- - C(4)	89(1)	I(6) - - C(6)	89(1)	88(1)
I(2)- ...I(3)	86(1)	I(4)- ...I(4)	85(1)	I(6) - ...I(1)	95(1)	
I(2)- ...I(6)	88(1)	I(4)- ...I(5)	96(1)	I(6) - ...I(6)	93(1)	

Intermolecular I···I contacts (< 4.35Å†)

I(1)···I(2)[5]	3.978
I(1)···I(5)[6]	4.241
I(2)···I(5)[6]	4.250
I(3)···I(4)[7]	3.948

‡ Thermal motion corrected values, see text.

† Van der Waal radii for Te=2.20 and I=2.15Å.

* Symmetry relationship (1) x,y,z; (2) $\bar{x},\bar{y},\bar{z}$; (3) $\bar{x},\bar{y}-1,\bar{z}$; (4) x,y,z+1 (5) x+1,y,z; (6) $x,\frac{1}{2}-y,\frac{1}{2}+z$; (7) x-1,y,z.

TABLE XIV. Measured and Calculated Structure Factors of α-$(CH_3)_2TeI_2$

scale = 1 x $F_{absolute}$

The origin for the F's in this table is different from that described in the text (section 3.6.3, first paragraph)

$-F_{obs}$ indicates unobserved reflexion

3.6.4 Structure Analysis of $f_4farsMn_2(CO)_8$

Of the 1540 independent intensities measured, 1349 were above 2σ and were considered as observed. The systematic absences were consistent with both the centrosymmetric Pnam and the noncentrosymmetric $Pna2_1$ space groups. The anomalous scattering of the arsenic and manganese atoms will cause break-down of Friedel's law[37] if the crystal belongs to a noncentrosymmetric space group. theory, this phenomenon can then be used to identify unambigously the true point group of the crystal. In practice, this would mean precise measurement of the reflexions most affected by anomalous scattering[37], although ideally both the hkl and $\bar{h}\bar{k}\bar{l}$ reflexion intensities should be obtained. In this structure, the distinction between the Pnam and $Pna2_1$ space groups was made through the Patterson map(as described in 3.2.3). The two arsenic and two manganese atomic positions obtained from the Patterson map were used in structure factor calculations (R=0.202). A Fourier electron density map revealed all the remaining non-hydrogen atoms and R decreased to 0.157. Two cycles of least-squares refinement(with unit weights) using isotropic temperature factors for all atoms brought R down to 0.082. At this point, the temperature factors of a carbonyl group had refined to ridiculous values showing that it was misplaced. Correction of these atomic positions led to an R of 0.063. An electron density difference map revealed the positions of the twelve hydrogen atoms as well as evidence for anisotropic thermal

motion about all the manganese, fluorine and oxygen atoms. Introducing the appropriate variables (positional and thermal parameters of the hydrogen atoms were not refined) brought R down to 0.038 and refinement stopped.

At this stage, the enantiomorph (with z changed to -z) was considered. The R factor improved to 0.35 with an overall increase in consistency among the As-C bond lengths . The improvement was significant* showing that this was the correct structure. The weighting scheme used during the final stages of refinement followed (20) with final numerical values of A=√1.93, B=27.30 and C=86.30. A final electron density difference map showed no variations larger than $\pm$ 0.39e/Å^3 (σ=0.20e/Å^3), the largest peak being 1.38 and 1.56Å away from O(8) and H(32), the largest trough being 0.990 and 0.724Å from the F(4) and C(16) atoms.

The molecular and unit cell packing diagrams are shown in Figures (5) and (6). Table (XV) lists the final atomic coordinates, Table (XVI) the interatomic distances and angles, Table (XVII) the mean plane equations, and Table(XVIII) the structure factor moduli and phases.

* The R factor ratio was 1.086(1,1439, 0.01) as compared to the listed value of 1.007(1,480,0.01).

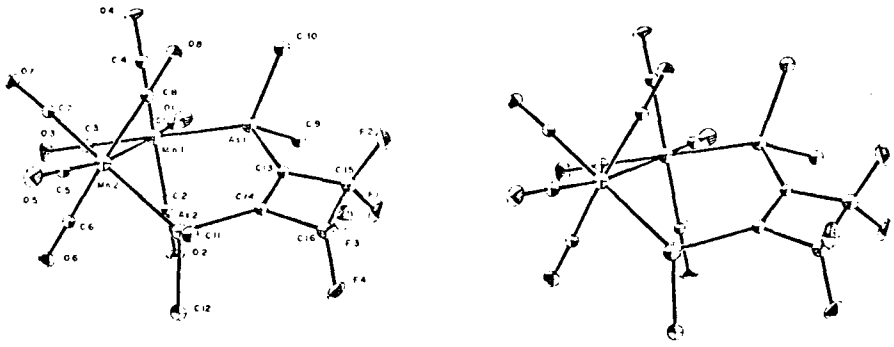

Figure 5. Stereo Diagram of $f_4farsMn_2(CO)_8$
The thermal ellipsoids (except those of As and Mn atoms which are not to scale) contain 8% electron density of the atoms.

Figure 6. Unit Cell Packing Diagram of $f_4farsMn_2(CO)_8$ viewed down c

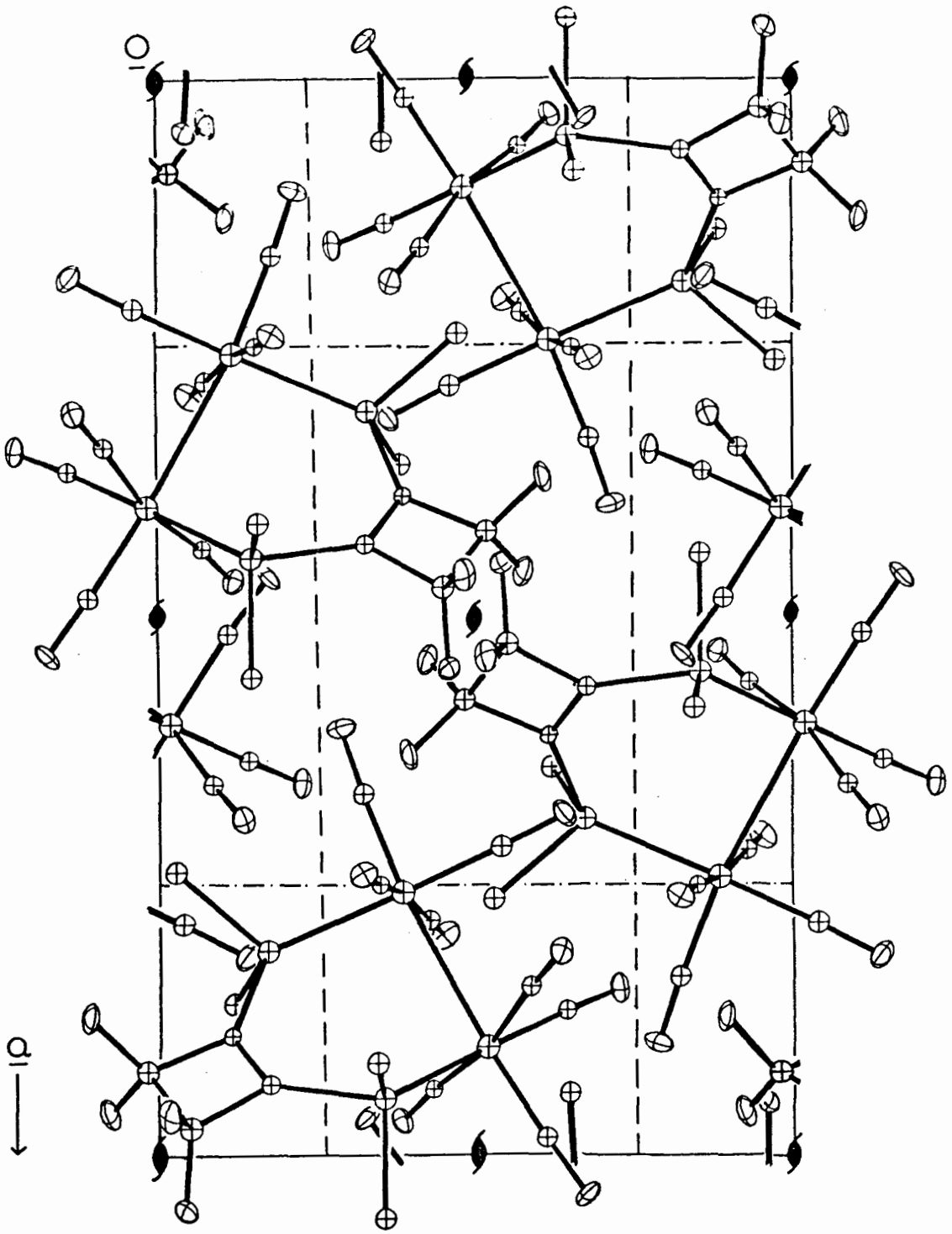

TABLE XV

Positional and Thermal Parameters for $f_4 fars Mn_2(CO)_8$

Atom		x	y	z	$B(\text{Å})^2$
As	1	0.3109(1)	0.3287(1)	0.7500	*
As	2	0.4472(1)	0.1461(1)	0.9574(1)	
Mn	1	0.2568(1)	0.1160(2)	0.7753(2)	
Mn	2	0.3994(1)	-0.0182(1)	0.8417(2)	
F	1	0.3720(5)	0.6069(7)	0.9118(8)	
F	2	0.4590(5)	0.5767(7)	0.7918(8)	
F	3	0.5493(5)	0.4584(8)	0.9338(9)	
F	4	0.4621(6)	0.4838(8)	1.0528(7)	
O	1	0.1039(5)	0.2143(11)	0.7203(9)	
O	2	0.2403(6)	0.1783(10)	1.0027(7)	
O	3	0.1840(6)	-0.1402(10)	0.8086(11)	
O	4	0.2957(6)	0.0493(11)	0.5544(8)	
O	5	0.5367(6)	-0.1729(10)	0.8869(9)	
O	6	0.3121(6)	-0.1333(9)	1.0202(8)	
O	7	0.3452(6)	-0.2245(8)	0.6995(8)	
O	8	0.4672(5)	0.1188(8)	0.6592(8)	
C	1	0.1649(7)	0.1792(13)	0.7401(12)	4.4 ‡
C	2	0.2498(7)	0.1521(11)	0.9153(9)	3.3
C	3	0.2140(7)	-0.0405(13)	0.7977(11)	4.8
C	4	0.2825(7)	0.0728(12)	0.6404(11)	4.0
C	5	0.4838(7)	-0.1093(12)	0.8691(10)	4.2
C	6	0.3433(7)	-0.0851(11)	0.9507(11)	3.9
C	7	0.3657(6)	-0.1424(11)	0.7555(10)	3.9
C	8	0.4379(6)	0.0691(11)	0.7311(9)	3.3
C	9	0.2376(7)	0.4736(12)	0.7704(9)	5.0
C	10	0.3600(8)	0.3812(14)	0.6200(11)	4.9
C	11	0.5577(7)	0.1461(12)	0.9710(12)	4.6
C	12	0.4151(8)	0.1570(13)	1.1053(11)	5.0
C	13	0.3881(6)	0.3859(10)	0.8477(10)	3.2
C	14	0.4334(6)	0.3249(12)	0.9169(9)	3.7
C	15	0.4216(7)	0.5180(14)	0.8693(11)	4.8
C	16	0.4736(8)	0.4501(14)	0.9500(13)	5.5
H	11	0.275	0.515	0.750	†
H	12	0.221	0.436	0.706	
H	13	0.225	0.450	0.830	
H	21	0.404	0.342	0.600	
H	22	0.370	0.485	0.630	
H	23	0.330	0.345	0.570	
H	31	0.565	0.200	1.019	
H	32	0.565	0.047	0.988	
H	33	0.571	0.145	0.570	
H	41	0.361	0.189	1.084	
H	42	0.422	0.076	1.113	
H	43	0.448	0.211	1.138	

(table XV continued)

Anisotropic thermal parameters

		U_{11} ($Ux10^4 Å^2$)	U_{22}	U_{33}	U_{12}	U_{13}	U_{23}
As	1	386(6)	342(5)	349(7)	23(5)	-40(6)	68(6)
As	2	378(6)	347(5)	310(6)	26(5)	-50(6)	21(6)
Mn	1	374(8)	429(9)	407(10)	-4(7)	-21(8)	-15(8)
Mn	2	483(9).	325(8)	389(9)	34(8)	10(8)	8(9)
		$Ux10^3(A^2)$					
F	1	116(7)	40(4)	137(9)	17(5)	-28(6)	-28(5)
F	2	117(7)	55(5)	118(8)	-30(5)	-13(6)	23(5)
F	3	67(5)	70(5)	152(9)	-9(5)	-31(6)	-9(5)
F	4	142(9)	69(6)	81(6)	-2(6)	-43(6)	-30(5)
0	1	52(6)	117(9)	101(9)	21(6)	-15(6)	-7(7)
0	2	87(7)	102(8)	41(5)	15(6)	13(5)	-4(5)
0	3	94(8)	71(7)	144(12)	-36(6)	20(8)	-3(7)
0	4	95(7)	117(8)	45(5)	28(7)	00(5)	-30(6)
0	5	75(7)	84(7)	96(8)	48(6)	-28(6)	-10(6)
0	6	91(7)	71(6)	71(6)	4(6)	29(6)	14(6)
0	7	113(8)	47(5)	63(6)	-7(5)	-16(6)	-8(5)
0	8	80(6)	62(6)	59(5)	-12(5)	17(5)	3(5)

* Anistropic temperature parameters for As 1 to 0 8 inclusive.
† Temperature factors for the hydrogen are $7.25Å^2$.
‡ Standard errors for the isotropic thermal parameters of the C atoms are $0.03(Å)^2$.

TABLE XVI Interatomic Distances and Angles for $f_4farsMn_2(CO)_8$

(A) Bonded Distances (Å)

Mn(1)-Mn(2)	2.972	C(13)-C(14)	1.34
Mn(1)-As(1)	2.405*	C(13)-C(15)	1.50
Mn(2)-As(2)	2.392*	C(14)-C(16)	1.53
Mn(1)-C(1)	1.79	C(15)-C(16)	1.54
C(2)	1.79	F(1)	1.37
C(3)	1.83	F(2)	1.33
C(4)	1.80	C(16)-F(3)	1.34
Mn(2)-C(5)	1.79	F(4)	1.37
C(6)	1.78		
C(7)	1.83	C(1)-O(1)	1.15
C(8)	1.80	C(2)-O(2)	1.15
As(1)-C(9)	1.98	C(3)-O(3)	1.16
C(10)	1.94	C(4)-O(4)	1.14
C(13)	1.93	C(5)-O(5)	1.16
As(2)-C(11)	1.94	C(6)-O(6)	1.15
C(12)	1.96	C(7)-O(7)	1.16
C(14)	1.93	C(8)-O(8)	1.16
		$0.82 \leq$ C-H ≤ 1.09	

Standard errors in bond length being 0.002Å for the Mn-Mn and Mn-As bonds and 0.02Å for the Mn-C, As-C, C-C, C-F and C-O bonds.

* These are corrected for thermal riding motion of the As on the Mn atoms. The uncorrected values are 2.403 and 2.389Å respectively.

TABLE XVI continued B. Bond Angles (°)

	Mn(1)*			Mn(2)*			As(1)*			As(2)*		
As(1)	Mn(2)	97.44	As(2)	Mn(1)	98.05	Mn(1)	C(9)	114.3	Mn(2)	C(11)	113.7
	C(1)	89.4		C(5)	87.8		C(10)	122.8		C(12)	122.0
	C(2)	88.4		C(6)	89.2		C(13)	117.8		C(14)	117.8
	C(3)	177.9		C(7)	178.9	C(9)	C(10)	100.8	C(11)	C(12)	122.0
	C(4)	90.0		C(8)	89.9		C(13)	98.0		C(14)	98.6
Mn(2)	C(1)	171.6	Mn(1)	C(5)	173.8	C(10)	C(13)	98.9	C(12)	C(14)	99.6
	C(2)	84.5		C(6)	86.5						
	C(3)	84.7		C(7)	83.1		C(15)*			C(16)*	
	C(4)	88.3		C(8)	81.9						
C(1)	C(2)	96.3	C(5)	C(6)	95.6	C(13)	C)16)	86.1	C(14)	C(16)	85.8
	C(3)	89.5		C(7)	91.0	F(1)	F(2)	107.6	F(3)	F(4)	105.9
	C(4)	94.2		C(8)	96.1	F(1)	C(13)	115.3		C(15)	117.8
C(2)	C(3)	90.0	C(6)	C(7)	91.1		C(16)	114.4		C(15)	116.9
	C(4)	169.3		C(8)	168.2	F(2)	C(13)	117.8	F(4)	C(14)	114.2
C(3)	C(4)	91.9	C(7)	C(8)	90.0		C(16)	114.2		C(15)	115.9

Standard errors in angles are:

As-Mn-Mn	=0.06	C-As-C	= 0.6
As-Mn-C	)	C-C-C	= 1.0
Mn-As-C	)0.4	F-C-C	≤ 1.3
Mn-Mn-C	)	F-C-F	≤ 1.2
		Mn-C-O	≤ 1.4

Mn(1)	- C(1) - O(1)		176.2
	- C(2) - O(2)		175.3
	- C(3) - O(3)		176.9
	- C(4) - O(4)		176.8
Mn(2)	- C(5) - O(5)		177.2
	- C(6) - O(6)		175.2
	- C(7) - O(7)		178.6
	- C(8) - O(8)		174.8
C(13)	- C(14) - C(16)		93.3
C(14)	- C(13) - C(15)		94.2

* denotes apex atom

Table XVI continued

(C)Selected intramolecular non-bond contacts (Å)

As(1),	As(2)	4.018	C(1),	C(2)	2.69
	Mn(2)	4.057		C(3)	2.52
	C(1)	2.98		C(4)	2.65
	C(2)	2.98	C(5),	C(6)	2.54
	C(4)	3.02		C(7)	2.68
				C(8)	2.66
As(2),	Mn(1)	4.065			
	C(5)	2.93			
	C(6)	2.99	C(2),	C(6)	2.97
	C(8)	3.00	C(3),	C(6)	3.02
				C(7)	2.90
F(1),	F(2)	2.18	C(4),	C(7)	3.02
	F(3)	2.70		C(8)	2.95
	F(4)	3.18			
F(2),	F(3)	2.69			
	F(4)	3.39			
F(3),	F(4)	2.16			

(D) Intermolecular non-hydrogen contacts (≤3.3Å)

Atoms	Distance	Symmetry Relationship
F(3), C(10)	3.29	1-x, 1-y, 1/2+z
O(1), O(8)	3.04	x-1/2, 1/2-y, z
O(2), O(7)	3.08	1/2-x, 1/2+y, z-1/2
O(6), C(10)	3.27	1/2-x, 1/2+y, z-1/2

TABLE XVII. Mean Planes for $f_4farsMn_2(CO)_8$

Equation*	Atoms	χ^2
(0.6849)x + (-0.1465)y +(-0.7137)z - (-3.6240)=0	C(13) C(14) C(15) C(16)	0.2674
(0.1840)x + (-0.2326)y +(-0.9550)z - (-8.8911)=0	A(1) M(2) C(1) C(3)	0.6580
(0.6988)x + (-0.1074)y +(-0.7072)z - (-3.3079)=0	A(1) A(2) C(13) C(14)	0.0194
(0.6923)x + (-0.1215)y +(-0.7113)z - (-3.4301)=0	A(1) A(2) C(13) C(14) C(15) C(16)	11.0414

*The coordinates are referred to the orthogonal axes of the unit cell in Å

TABLE XVIII. Measured and Calculated Structure Factors for $f_4farsMn_2(CO)_8$

scale = 1 x $F_{absolute}$

$-F_{obs}$ indicates unobserved reflexion

CHAPTER 4

RESULTS AND DISCUSSION

This section is divided into four parts, each of which is devoted to a discussion of the structural and chemical interest of each compound. The compounds containing transition metals, (I) and (IV), will be discussed before the main group compounds (II) and (III).

4.1 $(C_5H_5)_2Cr_2(NO)_3(NH_2)$

The molecule has an overall crystallographic mirror symmetry with the disordering of the two bridging NH_2 and NO groups. Because of the crystallographic problems described in section 3.6.1, one cannot distinguish whether the structure is in fact non-centrosymmetric with no crystallographic mirror plane of symmetry or alternatively is disordered as described. In addition, there is an approximate (non-crystallographic) twofold symmetry axis normal to the mirror plane and passing through the mid-point of the Cr-Cr vector.

The answer as to whether a direct metal-metal bond exists is not altogether clear-cut from consideration of the bond length and angles. The short Cr-Cr distance, 2.650Å, can be interpreted as evidence for a bond, but may also result from the imposed geometry. The values of the angles Cr(1)-N(3)-Cr(2) and N(3)-Cr-N(3) (86.4 and 93.1°) do not indicate decisively a net attractive force

between the metal atoms. Electronically however, the molecule may be formally considered as derived from two $C_5H_5^-$ moieties, two NO^+ (terminal) groups, an NO^- (bridging) group, an NH_2^- ion and two chromium(I) atoms; the formation of a metal-metal bond would therefore satisfy the EAN rule. It has also been recognized[38] that both the low oxidation states of the metal and high field ligands such as carbonyl and nitrosyl groups would help confer stability on metal-metal bonds. It has been proposed[38] that the influence of these high field ligands is mainly due to a π-effect. For instance, in an octahedral field the nonbonding t_{2g} orbitals in the metals have a decreased repulsion from each other if carbonyl or nitrosyl groups are present to withdraw electrons to their vacant π^* orbitals.

The bonding scheme of $(C_5H_5)_2Cr_2(NO)_3(NH_2)$ can be described in valence bond terms. To a first approximation let the Cr(1)-N(3)-Cr(3)-N(3)' fragment be planar. With say, Cr(1), as origin, the z-axis is chosen along the terminal nitrosyl group and the two bridging nitrogen atoms define the X and Y directions (the N(3)-Cr-N(3) angle being 93.1° is close to 90°). To bond with the cyclopentadiene carbon (C_5H_5 is treated as tridentate), terminal and bridging nitrogen atoms, each chromium atom utilizes the octahedral bridization of s, p_x, p_y, p_z, $d_{x^2-y^2}$, d_{z^2} orbitals; the two octahedra sharing an edge occupied by the two bridging

nitrogen atoms. A σ Cr-Cr bond is then formed by the unpaired electrons occupying the two d_{xy} orbitals. The fact that the two Cr-N(bridging)-Cr planes are folded about the Cr-Cr bond having a dihedral angle of 10.30° may be a result of the repulsion between the Cr-N(bridging) and Cr-Cr bonds.

Bush and his co-workers have studied compounds [40] with substituted amido bridging groups, cis- and trans-di-μ-dimethylamido-bis(cyclopentadienylnitrosylchromium(I), $[(C_5H_5)Cr(NO)NMe_2]_2$. Similar molecular geometry is found as in the present compound. From those isomers, they obtained single bond lengths of ~2.00Å for the Cr-NMe_2(bridging) bonds (σ character only). In the present compound, the Cr-N (bridging) bond determined is an average value of the Cr-NO and Cr-NH_2 bonds. The Cr-NO bond would be expected to be slightly shorter than a Cr-NH_2 or Cr-NMe_2 bond for two reasons. (i) The nitrogen atom is in an sp^2 hybridized state in the bridging NO group instead of sp^3, and thus it has a correspondingly smaller covalent radius. (ii) The more electronegative substituent, an oxygen atom, on the nitrogen atom will shorten the Cr-NO bond[61]. This is consistent with the Cr-N(bridging) bond lengths observed in $(C_5H_5)_2Cr_2(NO)_3(NH_2)$, 1.94(1)Å, which are therefore single bonds. The postulation of the bridging nitrosyl group as $N{=}O^-$ is also supported by the N=O (bridging) bond length of 1.12(2)Å. Unfortunately, structural data on

bridging nitrosyl compounds are rare(no other binuclear compound with bridging nitrosyl groups has been reported although a trinuclear manganese compound is known[62]), and few comparison can be made.

In contrast to the bridging bonds, the terminal Cr-N and N-O distances are 1.65(2)Å and 1.20(2)Å respectively indicating substantial multiple bond character. Similar values have been obtained in $[(C_5H_5)Cr(NO)N(Me)_2]_2$. This is achieved presumably through the filled d_{yz} and d_{xz} orbitals of the Cr atoms donating to the π^* orbitals of the nitrosyl groups.

The Cr-N-O(terminal) angles of 171.7(2.4) and 172.6(2.5)° show that the nitrosyl groups are barely significantly bent. This may be due to (i) crystal packing forces and non-bonding contacts of the terminal and bridging oxygen atoms (ii) unequal participation of the π^* orbitals of the NO groups in bonding with each metal atom as shown by Kettle [41]. The latter effect may be increased specially in the case when a distorted octahedral environment is found around the metal atom.

The mean chromium-carbon and carbon-carbon distances are 2.24(5)Å (range 2.16-2.31Å) and 1.43(11)Å (range 1.30 to 1.50Å) respectively. The accuracy is rather low but they are in the range found in chromium-containing structures of a similar type[42]. (Moreover

least-squares planes in Table (V) show the rings deviate from planarity.) It has been suggested[42] that when the cylindrical symmetry around the metal atom is destroyed, as in the present compound, the C-C distances may not be all precisely equal and distortions from a perfectly π-bonded cyclopentadiene ring can occur. The two disordered orientations make an angle of less than 3° between themselves. The rings are non-parallel and subtend an angle of at least 5° (taking planes nearest parallel in pairs). This non-parallelism can be explained by one or a combination of the following factors : (i) the slight folding of the Cr-N(bridging)-Cr planes has caused the two octahedra around the chromium atoms to have non-parallel faces (ii) in the parent molecule it is possible that the NO and NH_2 groups will not allow mirror symmetry and thus provide an asymmetric electronic distribution about the chromium atoms and cause a different tilt for each of the C_5H_5 rings.

4.2 $(f_4fars)Mn_2(CO)_8$

In the $(f_4fars)Mn_2(CO)_8$ molecule, each manganese atom is bonded to four carbonyl groups and an arsenic atom of the f_4fars ligand. The EAN rule is satisfied by considering each CO group and arsenic atom as two electron-donors, and the unpaired electron of the formally zero-valent manganese atom pairing up in a metal-metal bond. The present compound can be well described as a derivative of the parent compound $Mn_2(CO)_{10}$ with one CO group displaced on each manganese atom by an arsenic atom of the f_4fars ligand. The ligands about the Mn-Mn bond are staggered, forming a distorted octahedral environment about each manganese atom. The molecule has an approximate noncrystallographic two-fold axis of symmetry, which passes through the mid-points of the Mn-Mn and As...As vectors, as shown in Figure 7.

The Mn-Mn bond in $Mn_2(CO)_{10}$[15] has been determined to be 2.923(3)Å, a value much longer than would be predicted from Pauling's value of the covalent radius for the manganese atom, 1.2Å[48]. Since there is no bridging group present in $Mn_2(CO)_{10}$, the molecule can be expected to have direct metal-metal interaction , which is also supported by the thermodynamic studies indicating an interaction of considerable strength[44]. The Mn-Mn bond is thus unlikely to have been stretched by 0.5Å. Clearly the first order approximation of Pauling's covalent radius is not

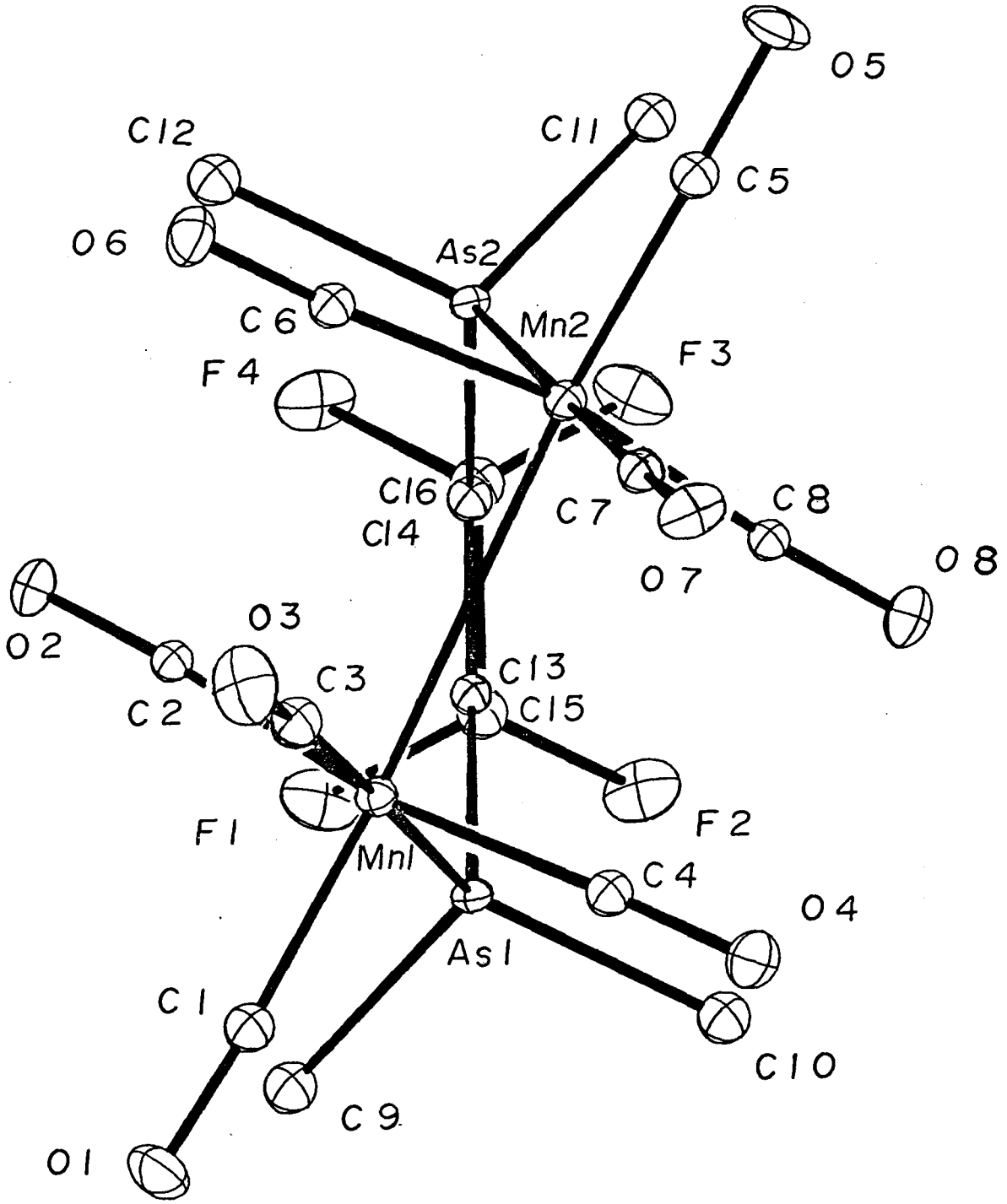

Figure 7. Projection of $f_4farsMn_2(CO)_8$ down the approximate Two-fold symmetry axis. Thermal ellipsoids contain 8% of the electron density of the atoms.

appropriate for the manganese atom in this compound and attempts have been made to assign a satisfactory covalent radius for Mn(0)[45,39], the best values being 1.39-1.43Å , not too different from the experimental result. Furthermore, a molecular orbital scheme set up by Bennett and Mason[46] is able to explain the lengthening of the Mn-Mn bond up to 0.1Å, taking into account that the hybrid orbitals used in metal-metal bond formation have greater "p" and "d" character. Hence the Mn-Mn bond may be regarded as quite "normal" under the circumstances. The Mn-Mn bond found in $f_4farsMn_2(CO)_8$ is longer by about 0.05Å and there can be two reasons for this. (i) Compared to a CO group, the arsenic atom in the $f_4$fars ligand is a good σ donor but is a poor π acceptor. This is consistent with the observation that while high π-interacting ligands tend to stabilize a metal-metal bond, substitution with low π-interacting ligands tend to destabilize it (Section 4.1). (ii) The $f_4$fars ligand is relatively "bulky". It has been observed that a bridging ligand containing higher row element or more than one bridging element tend to be associated with a longer metal-metal bond (for instance, the Fe-Fe bond in $Fe_2I_2(NO)_4$ where the Fe atoms are bridged by iodine atoms have a Fe-Fe bond of 3.05Å[47]). In other words, both the electronic and geometric factors of the $f_4$fars ligand work towards a longer Mn-Mn bond.

The two sets of non-terminal carbon atoms C(2), C(3), C(4) and C(6),C(7),C(8) are bent inwards towards each other as seen from the acute angles they make with the Mn-Mn bond vector. Similar bending was observed in $Mn_2(CO)_{10}$ which was attributed to the non-bonding repulsion between these non-terminal and the terminal carbon atoms as suggested by their non-bond contacts[15]. (The molecular orbital scheme of Bennett & Mason[46] tied the bending-in of the CO groups with the lengthening of the Mn-Mn bond elegantly.) The arsenic atoms in $f_4farsMn_2(CO)_8$, however, are situated away from the Mn-Mn bond, having a mean Mn-Mn-As angle of 97.75 (presumably with a mean Mn-As bond length of 2.399Å the non-bond repulsion between the terminal carbon and the arsenic atoms are negligible). The bite of the As...As atoms has been found to depend largely on the mode of ligation. For instance, it is 3.223Å in $f_4farsFe_2(CO)_6$[48] where the As atoms are both bonded to the same Fe atom(while the C=C bond is π-bonded to the other Fe atom), 4.31Å in $f_4farsMn_2(CO)_8I_2$[14] where there is no Mn-Mn bond and a bridging $f_4$fars ligand is reponsible only for holding the two $Mn(CO)_4I$ moieties together, 4.108 in $(f_4fars)_2Ru_3(CO)_8$[49] and 4.018(3)Å in the present compound where each $f_4$fars ligand links two metal atoms that form a metal-metal bond.

The arsenic atoms and the cyclobutene ring are coplanar (Table XVI). All the As-C bonds are equivalent within stand-

ard errors. From the C-As-C and C-As-Mn angles it can be seen that the lone pair positions are in the As-Mn bond directions. The double-bond in the cyclobutene ring C(13)=C(14) has an expected value of 1.34(2)Å and the remaining C-C bonds lie within the range of 1.50-1.54(2)Å as expected for single C-C bonds. The C-C-C angles in the ring deviate from 90° as expected from the different geometry of sp^2 and sp^3 hydridizations. The C-F bonds (mean value 1.35Å) also compare well with those found in other $f_4$fars ligand containing compounds.

The Mn-C and C-O bonds range from 1.78 to 1.83 and 1.14 to 1.16Å respectively. No significant variations are found amongst these distances. All the Mn-C-O atoms are colinear.

4.3 $KIO_3.HIO_3$

Each iodine atom is covalently bonded to three oxygen atoms at distances ranging from 1.753 to 1.952Å apart, forming a distorted trigonal pyramidal arrangement. In addition extensive oxygen-iodine contacts ranging from 2.4 to 3.4Å(sum of van der Waals radii for iodine and oxygen atoms being 3.5Å) exist between neighbouring iodate ions. As a result, the iodine atoms have two types of environments. I(1),I(3), and I(4) are each surrounded by oxygen atoms forming a distorted octahedron. Similar situations have been found in a number of iodate compounds[7]. I(2), however, has a highly distorted capped-octahedral environment with four distant I...O contacts. Two of these interactions arise from a crystallographically equivalent (centro-symmetrically related, I(2)) iodate ion; and the remaining two from other independent iodate ions.

Among the twelve independent I-O bonds (Table IXA), two stand out to be significantly longer than the rest, namely I(4)-O(42)=1.952 and I(3)-O(32)=1.911Å. These are expected to be the hydroxylic oxygen atoms (peaks at suitable positions for hydrogen atoms were found in the final electron density difference map but they were no higher than spurious non-atomic peaks). Further support for this interpretation are the distances O(42)-O(32)=2.708 and O(42)-O(11)=2.731Å which are the only O-O distances less than 2.80Å between

different iodate groups. Also this is fully consistent with the O-H stretching frequency in the reported infrared spectrum[6] which would predict an OH-O length of 2.7Å on the basis of existing empirical correlations[50]. From these I-O and O-O distances, one may conclude that O(43) acts both as a hydrogen bond donor and acceptor whereas O(32) acts only as a hydrogen bond donor. The interatomic angles computed for this hydrogen bonding scheme (Table IXD) show reasonable agreement.

Formal bond orders can be assigned to the different I-O bonds, for instance, a value of 1 to O_2I-OH, $1\frac{2}{3}$ in IO_3^- ions and 2 to HOI-O_2. Results in Table IXB show that while bonds of order 1 are significantly different from those of order $1\frac{2}{3}$, there is no substantial difference between those of the latter and those of bond order of 2. Bond length variations between bond orders of $1\frac{2}{3}$ and 2 are expected to be small in any event, especially when variations in the extensive weak I...O interactions may further mask these fractional differences.

To account for the interionic interactions, the electronegative environment of the iodine atom is probably responsible for contraction of the empty 5d orbitals allowing them to provide suitable overlap with the oxygen filled p orbitals, as pointed out by Mitchell[51]. Furthermore, for the XO_3^- species, one would expect the acceptor strength to

increase in the order of X=Cl,Br,I, as I is the most polarizable and thus has the highest effective positive charge.

The lengths of the weak I...O contacts are strikingly different for the IO_3^- and HIO_3 moieties. The average I...O distances are invariably longer for the IO_3^- ions (involving I(1) and I(2)) than the HIO_3 species (involving I(3) and I(4)). (See Table IXB.) An explanation may be found in terms of a more electrophilic iodine atom in HIO_3 to accept electrons.

The lone-pair on the iodine atom may be proposed to be situated in between the longer I...O contacts in the case of the distorted octahedral environment. However, a head-on approach of an oxygen atom directly towards a lone pair position as is found in a regular capped-octahedron will not be expected. In fact, the line of approach of the distorted capped oxygen atom O(31) to I(2) is considerably displaced towards one side of the triangle formed by O(21)', O(22)' and O(13). It can thus be inferred that the lone pair of electrons in I(2) may have a higher s character.

Each potassium ion has eight near-neighbouring oxygen atoms with K-O distances ranging from 2.67 to 3.04Å and has an environment best described as a distorted square antiprism. The squares around K(1) consist of O(21), O(22), O(23), O(41) and O(13), O(43) O(23)', O(13)' while those around K(2) consist of O(31), O(41), O(32), O(42) and O(21), O(12), O(33), and O(11).

Earlier work[52] by Rogers and Helmholz on α-HIO_3 led them to believe the structure to consist of bifurcated hydrogen bonds. Wells[8] however, re-examined the structure and concluded that it should be described as infinite $HIO_3...HIO_3...$ chains; this model was confirmed by Garrett's[8] neutron diffraction work. The overall structure of $KIO_3.HIO_3$ may be considered to consist of $(IO_3...HIO_3...HIO_3)^-$, $(IO_3...IO_3)^=$ and K^+ ions packed together electrostatically. However the geometry of the $(IO_3...HIO_3...HIO_3)^-$ moiety differs substantially from a fragment of the infinite $HIO_3...HIO_3...$ chain proposed by Wells as it involves the same oxygen atom O(42) twice.

Considerable interest has been found in the structures of HX_2^- anions[63] (e.g. X= NO_3, CO_3, RCOO). Writing the formula of $KIO_3.HIO_3$ in the form $K^+H(IO_3)_2^-$, one might expect the compound to provide a similar HX_2^- system. However, the crystal structure of $KIO_3.HIO_3$ clearly shows that it has a hydrogen bonding scheme which is quite distinctly different from that which was found in $H(NO_3)_2^-$ [63,64], $H(CO_3)_2^-$ [63], and $H(RCOO)_2^-$ [63]. There is no discrete $H(IO_3)_2^-$ anion present. It is also noted that relationships[65] between O-H...O and O-H distances suggest an asymmetric hydrogen atom from the two oxygen atomic positions. This prediction is consistent with the proposed hydrogen bonding scheme.

Thermal motion for the different atoms in $KIO_3.HIO_3$ is generally low (although they may contain errors due to approximate absorption corrections, the values obtained are reasonable), a fact which may be attributed to the

ionic nature and the hydrogen bonding present giving a stable 3-dimensional structure. It is also consistent with the high density, the hardness and difficulty in cleaving the crystals. The packing density of oxygen atoms in $KIO_3.HIO_3$ is less than that found for other structures containing the iodate ion[53]. The volume per oxygen atom is 26$\mathring{A}^3$ compared to about 16 in a closest-packed structure.

It has been found that a sample of $KIO_3.HIO_3$ exhibits a strong second harmonic effect[54] indicating that, as in the parent compounds KIO_3 and HIO_3, a crystallographic centre of symmetry is lacking. This agrees also with a recent report on the piezoelectric effect[55] of the same crystals. In this work, refinement in the possible non-centrosymmetric space group was not carried out because of two reasons. (i) From a chemical interest view point, the positions of the hydrogen atoms are not found in the present case , and probably will not be readily located either in the non-centrosymmetric case. (ii) Since the x-ray diffraction patterns conform so closely to those of the space group $P2_1/c$, the heavy atoms must be in almost perfectly centrosymmetric arrangement (this is also supported by the small anisotropy in their thermal motion). It is possible that the deviation from centrosymmetry arises mainly through the hydrogen bonding of the structure. Refinement in the noncentrosymmetric case will probably be complicated by a large number of interactions between parameters due to the pseudo-centrosymmetry. The present good agreement obtained really shows that $P2_1/c$ is a very close approximation to the true space group of the structure.

4.4 α-$(CH_3)_2TeI_2$

In the gaseous state, modern structural theory[56] might predict a trigonal bipyramidal geometry for $(CH_3)_2TeI_2$ with the lone pair of electrons and the methyl groups in a distorted trigonal plane, and the iodine atoms at the axial positions. In the solid state, however, an octahedral environment of varying regularity is found for each of the three crystallographically independent tellurium atoms, formed by two trans- Te-I bonds, two cis- Te-C bonds and two weak intermolecular Te...I contacts, as a result of which, the molecules are linked together in corrugated sheets approximately parallel to (010).

These weaker intermolecular interactions may be regarded as involving the partial donation and acceptance of electrons of the tellurium atoms with neighbouring iodine atoms. Such interactions have always been observed in a number of organo-tellurium halides, and the donor-acceptor role played by a tellurium atom is often critically determined by its environment. For instance, in the β-form of dimethyltellurium di-iodide, $[(CH_3)_3Te^+][CH_3I_4Te^-]$, the tellurium atom acts as a donor in the anion and an acceptor in the cation[11] . In the present compound, the same tellurium atom can be considered to be acting both as donor and acceptor, indicating that the factors governing these weak interactions are delicately balanced.

A comparison between the structures of α-$(CH_3)_2TeI_2$ and α-$(CH_3)_2TeCl_2$[57] shows that the two structures are somewhat similar. However, the iodide definitely assumes a more regular octahedral geometry in each of the three independent molecules. This can be explained by the electronegativity difference between the iodine and chlorine atoms, which have two main consequences. Firstly, the chlorine atom does not donate a lone pair of electrons readily and secondly, the $Te^{\delta+}$-$Cl^{\delta-}$ σ bond polarity decreases the donor power of the tellurium atom. Also it is worth noting that when the methyl groups are replaced by more electron-withdrawing aromatic systems (for example, in $(C_6H_5)_2TeBr_2$[58] and $(p\text{-}ClC_6H_4)_2TeI_2$[59]),the lone pair donor power of the tellurium atom is correspondingly reduced and fewer short intermolecular Te...X (X=I or Br) contacts result. For example, all Te...I contacts in reference 59 are >4.1Å.

The Te-I covalent bonds are found to be significantly longer than the sum of covalent radii 2.70Å [43] for the tellurium and iodine atoms and they also differ significantly amongst themselves (see the range of the Te-I bonds in Table XIII). The bond lengthening may be attributed to the polymeric Te...I linkages in the structure as well as a high participation of the Te d_{z^2} orbital in the Te-I bond formation; or alternatively, the Te-I bonds can be regarded as having a covalent bond order of less than one.

The variations of the Te-I bonds are also consistent with the different degrees of the intermolecular interactions. Thus I(6), whose Te(3)-I(6) bond is substantially longer than all the other Te-I bonds, is the only iodine atom that forms more than one interatomic contact , both to Te(1) and Te(3), and the Te(1)...I(6) value of 3.659(3)Å is the shortest of all. As a result of the long Te(3)-I(6) bond, the trans- ligand, I(5), may have an increased orbital overlap with Te(3) to give the shortest Te-I bond, 2.854(3)Å. Furthermore it is noted that the considerable lengthening of Te(1)-I(1) (2.965(3)Å), over Te(1)-I(2) (2.885(3)Å), is consistent with the fact that I(2) does not form any intermolecular Te...I contact.

The variations in lengths of the Te...I contacts also affect the regularity of the "square" plane formed by the methyl carbon and the weakly bonded iodine atoms, and they follow the order Te(3)≤Te(2)≪Te(1). A nearly regular octahedral arrangement of bond angles is formed in the case of Te(1). The wide range of the I...Te...I angles (Table XIII) as opposed to the relatively constant near-90° C-Te-C angles is consistent with the idea that more p character is associated with the Te-C bonds and more s character with the Te lone pair of electrons. Further support for this is found in the observation that only with the methyl groups in a cis- arrangement can each Te-C bond obtain the maximum possible p-character. A small positive ^{125}Te Mössbauer isomer shift[60] of +0.55(20)mm/sec (with respect to Cu^{125}I) is consistent with a

bonding scheme involving principally 5p and 5d orbitals of the Te atom.

The Te-C distances are in the range from 2.10 to 2.16(3)Å with a mean value of 2.14Å which is identical to the sum of covalent radii of 2.14Å for Te and C atoms. It may be noted that in α-$(CH_3)_2TeCl_2$ the mean Te-C bond obtained is 2.09(3)Å. Although the difference is not significant it is in the direction expected from a bond shortening effect due to the more electronegative tellurium substituents[61].

APPENDIX

The following page lists a program to compute the U_{ij}'s from the B_{ij}'s of the atoms, and the lower and upper bound limits of the bond lengths as given in equation (25).

The input cards required are as follows:

1. unit cell dimension , a,b,c,($\mathring{A}$);$\alpha,\beta,\gamma(^\circ)$, (6F10.6)
2. atom name (A6)
3. $B_{11},B_{22},B_{33},B_{12},B_{13},B_{23}$ ($\mathring{A}^2$) (6F10.6)
4. IEND, σ of B_{ij}'s in the same order as 3. (I1,F9.6,5F10.6)
   Cards 2,3,and 4 repeat for each atom, the last set should set IEND=1, otherwise IEND=0
5. R_1,R_2,R_3,R_4,SO (5F10.5)
   R_1 and R_3 are the r.m.s. radial thermal displacements for atoms A and B when the lower and upper bound limits of bond A-B are to be determined. R_2 and R_4 are the r.m.s. components of thermal displacement of A and B in the direction A-B. SO is the uncorrected bond length of A-B. These five values are available through ORFFE. One card is for one bond. More cards can be added if required.
6. One blank card.

```
      DIMENSION A(6),B(6),SB(6),R(4)
      READ(5,3)A,BB,C,ALP,BET,GAM
    3 FORMAT (6F10.6)
      RAD=.01745329
      COSA=COS(ALP*RAD)
      COSB=COS(BET*RAD)
      COSG=COS(GAM*RAD)
      SINA=SIN(ALP*RAD)
      SINB=SIN(BET*RAD)
      SING=SIN(GAM*RAD)
      FF=(1.0-COSA**2-COSB**2-COSG**2+2.*COSA*COSB*COSG)/19.7392
      D(1)=(FF*A*A)/(SINA**2)
      D(2)=(FF*BB*BB)/(SINB**2)
      D(3)=(FF*C*C)/(SING**2)
      D(4)=FF*A*BB/(SINA*SINB)
      D(5)=FF*C*A/(SING*SINA)
      D(6)=FF*BB*C/(SINB*SING)
      WRITE (6,8)       COSA,COSB,COSG,SINA,SINB,SING
    8 FORMAT (1H ,6F10.6)
      WRITE (6,7) FF
    7 FORMAT (1H ,F10.6)
      WRITE (6,6) (D(I),I=1,6)
    6 FORMAT (1H ,6F10.6)
   20 READ(5,1) ATOM
      READ (5,3) (B(I),I=1,6)
      READ(5,2) IEND,(SB(I),I=1,6)
    1 FORMAT (A6)
    2 FORMAT (I1,F9.6,5F10.6)
      DO 10 I=1,6
      B(I)=B(I)*D(I)
   10 SB(I)=SB(I)*D(I)
      WRITE (6,4)ATOM,(B(I),I=1,6)
    4 FORMAT (1H ,A6,6X,6F10.6)
      WRITE(6,5)(SB(I),I=1,6)
    5 FORMAT (1H ,12X,6F10.6)
      IF(IEND.EQ.1) GO TO 30
      GO TO 20
   30 READ (5,31) (R(I),I=1,4),SD
   31 FORMAT (5F10.5)
      IF(R(1).EQ.0.)GO TO 40
      DO 34 I=1,4
   34 R(I)=(R(I))**2
      DELTB=SQRT(R(1)-R(2))
      DELTA=SQRT(R(3)-R(4))
      WLSQ=SD+(((DELTB-DELTA)**2)/(2*SD))
      WUSQ=SD+(((DELTB+DELTA)**2)/(2*SD))
      WRITE(6,32) WLSQ,WUSQ
   32 FORMAT(1H ,2F10.5)
      GO TO 30
   40 CALL EXIT
      END
```

REFERENCE

1. M. Ahmad, R. Bruce and G. Knox, Z. Naturforsch., (B) 21, 289 (1966).
   M.A. Bush, G.A. Sim, G.R. Knox, M. Ahmad and C.G. Robertson, Chem. Comm., 74 (1969).
2. R.B. King and M.B. Bisnette, Inorg. Chem., 3, 791 (1964).
3. O.S. Mills, Acta Cryst., 11, 620 (1958).
   F.A. Cotton and G. Yagupsky, Inorg. Chem., 6, 15 (1967).
4. R.D. Fischer, A. Volger and K. Noack, J. Organometal. Chem., 7, 135 (1967).
5. N. Flitcroft, J. Organometal. Chem., 5, 254 (1968).
6. W.E. Dasent and T.C. Waddington, J. Chem. Soc. (A), 2429 (1960).
7. E.T. Keve, S.C. Abrahams and J.L. Berstein, J. Chem. Phy., 54, 2556 (1967).
8. B.S. Garrett, Struct. Rep., 18, 393 (1954).
   A.F. Wells, Acta Cryst., 2, 128 (1949).
9. R.H. Vernon, J. Chem. Soc., 86 (1920);
   R.H. Vernon, ibid. 106.(1921).
10. H.D.K. Drew, ibid., 560 (1929).
11. F. Einstein, J. Trotter and C. Williston, ibid.(A), 2019 (1967).
12. E.E. Galloni and J. Pugliese, Acta Cryst., 3, 319 (1950).
13. W.R. Cullen, Fluorine Chem. Rev.,3, 73 (1969).
14. a) J.P. Crow, W.R. Cullen and F.L. Hcu, private communication.
    b) Lilian Y.Y. Chan and F.W.B. Einstein, unpublished results.
15. R.E. Rundle and L.F. Dahl, Acta Cryst., 16, 419 (1963).
16. R.D. Burbank, ibid., 19, 957 (1965).
    P. Coppens, ibid., (A), 24, 253 (1968).

17. T.C. Furnas in "Single Crystal Orienter Instruction Manual", Milwaukee, Wis., Gen. Elec. Company (1957).

A.C.T. North, D.C. Philips and F.S. Mathews, Acta Cryst., A 24, 35 (1968).

18. J.A. Ibers and D.H. Templeton in "International Tables for X-Ray Crystallography", Vol. III, Section 3.3, Kynoch Press, Birmingham, England, 1962.

19. R.F. Stewart, E.R. Davidson, and W.T. Simpson, J. Chem. Phy., 42, 3175 (1965).

20. R.W. James in "The Crystalline State", Vol.II, Sir Lawrence Bragg, ed., G. Bell and Sons Ltd., London, England, 1965, p. 38-39.

J.M. Robertson in "Organic Crystals and Molecules", Cornell University Press, Ithaca, 1953, p. 89-92.

21. G.H, Stout and L.H. Jensen in "X-Ray Structure Determination", The Macmillan Company, New York, N.Y. , 1968, (a) p. 207-209 (b) p. 321.

22. J. Karle and I.L. Karle, Acta Cryst., 21, 849 (1966).

H. Hauptman and J. Karle in "ACA Monograph No. 3", Polycrystal Book Service, New York, N.Y., 1953.

23. W. Cochran and M.M. Woolfson, Acta Cryst., 8, 1 (1955).

24. F.R. Ahmed in "Crystallographic Computing", F.R. Ahmed, ed., Munksgaard, Coperhagen, Denmark, 1950, p. 55.

25. S. Hall, ibid., p. 66.

26. R.B.K. Dewar, ibid., p. 63.

27. H. Lipson and W. Cochran in "The Crystalline State", Vol.III, Sir Lawrence Bragg, ed., G. Bell and Sons Ltd., London, England, 1966, Chapter 7.

28. J.S. Rollet in "Computing Methods in Crystallography" J.S. Rollet, ed., Pergamon Press, New York, N.Y., 1965, p. 47.

29. D.W.J.Cruickshank,ibid., p. 217 (1965).

30. W.C. Hamilton in "Statistics in Physical Sciences", Ronald Press Company, New York, N.Y., 1964, p. 217.

31. M.J. Buerger in "X-Ray Crystal Structure Analysis", John Wiley & Sons, Inc., New York, N.Y., 1960, p. 202.

32. W.H. Zacharisen, Acta Cryst., 16, 1139 (1963).

33. C.K. Johnson in "Crystallographic Computing", see reference 24, p.220.

34. W.R. Busing and H.A. Levy, Acta Cryst., 17, 142 (1964).

35. V. Schomaker and K.N. Trueblood, ibid.,(B)24, 63 (1968).

36. S. Geller, Acta Cryst., 14, 1026 (1961).

37. S. Rachmaseshan in "Advanced Methods of Crystallography", G.N. Ramachandran, ed., Academic Press, London, England, 1964.

38. M.C. Baird, Progr. Inorg. Chem. 9, 122 (1968).

39. F.A. Cotton and C.C. Richardson, Inorg. Chem., 5, 1851 (1966).

40. M.A. Bush, G.A. Sim, G.R. Knox, M. Ahmad and C.G. Robertson, Chem. Comm., 74 (1969).
M.A. Bush,and G.A.Sim, J.Chem.Soc.,(A), 611 (1970).

41. S.F.Kettle, Inorg.Chem., 4, 1661 (1965).

42. P.J. Wheatley, Perspectives in Structural Chemistry, 1 27 (1967).

43. L. Pauling in "The Nature of the Chemical Bond", 3rd ed., Cornell University Press, Ithaca, N.Y., 1965, p. 256.

44. F.A. Cotton and R.R. Monchamp, J. Chem Soc., 533 (1960).

45. B.T. Kilbourm and H.M. Powell, Chem. and Ind., 37, 1578 (1964).

46. M.J. Bennett and R. Mason, Nature, 205, 760 (1965).

47. L.F.Dahl, E. Rodulfo de Gil and R.D. Feltham, J. Am. Chem. Soc., 91, 1653 (1969).

48. F.W.B. Einstein and J. Trotter, J. Chem. Soc.,(A),824 (1967).

49. P.J. Roberts and J. Trotter, ibid., 3246 (1970).

50. W.C. Hamilton and J.A. Ibers in "Hydrogen Bonding in Solids", Benjamin Inc., New York, N.Y. 1968, p. 87.
K. Nakamoto, M. Margoshes and R.E. Rundle, J. Am. Chem. Soc., 77, 6480 (1955).

51. K.A.R. Mitchell, Chem. Rev., 69, 157 (1969).

52. M.T. Rogers and L. Helmholz, J. Am. Chem. Soc., 63, 278 (1941).

53. J.A. Ibers, Acta Cryst., 9, 225 (1956).

54. K. Rieckhoff and R. Ninnis, private communication.

55. G. Kemper and Aafje Vos, Acta Cryst.,(B)26 , 302 (1970).

56. R.J. Gillespie, J. Am. Chem. Soc., 82, 5978 (1960).

57. G.D. Christofferson, R.A. Sparks and J.D. McCullough, Acta Cryst.,11, 782 (1958).

58. G.D. Christofferson and J.D. McCullough, ibid., 11, 249 (1958).

59. G.Y. Chao and J.D. McCullough, ibid., 15, 887 (1962).

60. R. Cheyne and C.H.W. Jones, private communication.

61. H.A. Bent, Chem. Rev., 68, 587 (1968).

62. O.S. Mills and E.F. Paulus, J. Organomet. Chem., 10, 331 (1967).

63. D.G. Tuck, Progr. Inorg. Chem., 9, 161 (1968).

64. B.D. Faithful and S.C. Wallwork, Chem. Comm., 1211 (1967).

65. G.E. Bacon in " Applications of Neutron Diffraction in Chemistry", Pergamon Press, New York,1963, p.47.